DuraMAT
Durable Module Materials Consortium

SAND2020-10430C

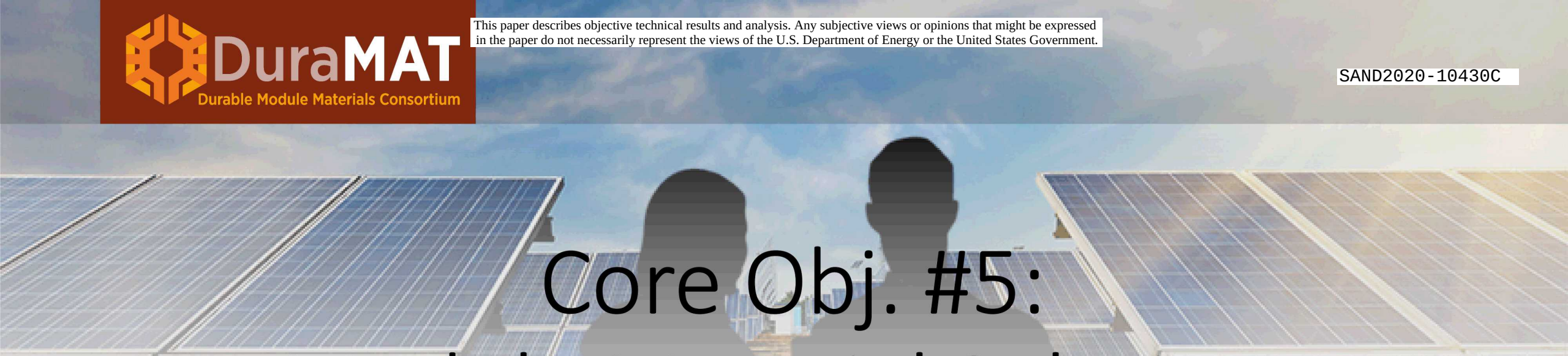

Core Obj. #5: Module Material Solutions

Sept. 23, 2020

Margaret Gordon (SNL)

PIs: Alan Lyons (CUNY), Sam Graham (Georgia Tech), Stuart Bowden (ASU), Zak Holman (ASU), Sang Han (Osazda), Kurt Durme-van (DSM), David Okawa (SunPower), Reinholdt Dauskardt (Stanford)

Sandia National Laboratories is a multimission laboratory managed and operated by National Technology & Engineering Solutions of Sandia, LLC, a wholly owned subsidiary of Honeywell International Inc., for the U.S. Department of Energy's National Nuclear Security Administration under contract DE-NA0003525.

Module Material Solutions

Design, develop, de-risk innovative materials and module architectures to address PV reliability issues using DuraMAT Capabilities

Key Results:

- De-risk innovative materials using accelerated testing and materials forensics:
  - characterization of failure modes in ECAs, develop crack tolerant metallization to increase reliability of cells, design sustainable, reliable, recyclable backsheets
- Enable new architectures including:
  - Flexible modules: define the technical requirement of each component in the flexible module as well as the overall material stack, and develop process to experimentally evaluate module performances, Advance reliability of bifacial modules through new transparent packaging materials

Materials Solutions Project List Current and Completed

1. Low-Cost Advanced Metallization to Reduce Cell-Crack-Induced Degradation for Increased Module Reliability – S. Han, Osazda
    1. *Low cost, crack tolerant metallization - Complete*
2. Advanced material development to support low-LCOE 25-year flexible photovoltaic modules – D. Okawa, SunPower
    1. *Development of Flexible Panel Front Sheet with Twenty-Five (25) Year Rated Lifetime -Complete*
3. Determination of PV Module Degradation Rates and their Correlation to Backsheets Material Properties: A Comparison of Market-Benchmark Technologies to Novel Non-Flouro-Based Co-Extruded Backsheet Materials – K. Durme-van, DSM
4. Advancing Bifacial Solar Module Reliability and Manufacturability with New Module Materials and Light-Weight Transparent Back Lamination – R. Dauskardt, Stanford
    1. *New Concepts for Reliable Low-Cost Module Encapsulation and Barrier Technologies - Complete*
5. *A Hybrid Hydrophobic-Hydrophilic Coating with combined AR/AS properties – A. Lyons (CUNY) Complete 2020*
6. *Scalable Packaging Materials for R2R thin film solar cells – S. Graham, (Georgia Tech) Complete 2020*
7. *Reliability of modules with high efficiency solar cells with copper contacts – S. Bowden (ASU) Complete 2020*
8. *Failure mechanisms in electrically conductive adhesive interconnects – Z. Holman (ASU) Complete 2020*
9. *Development of a Spray Deposition Method for a Polysilsequioxane Coating for PV Modules – C. Staiger (SNL) Complete*
10. *Establishing Structural Changes with Backsheet Degradation and Cracking – A. Colli (BNL) Complete*
11. *Discovering New Materials for PV Encapsulation – K. Barth, NGPV Complete*
12. *Advanced multifunctional coatings for PV glass to reduce soiling and PID losses – D. Fleming (Wattglass) Complete*
13. *Highly-conductive, Low-cost Polymer Adhesive Composites with Complex Dimensional Fillers – Zhu BAPVC Complete*

Materials Solutions Project Integration

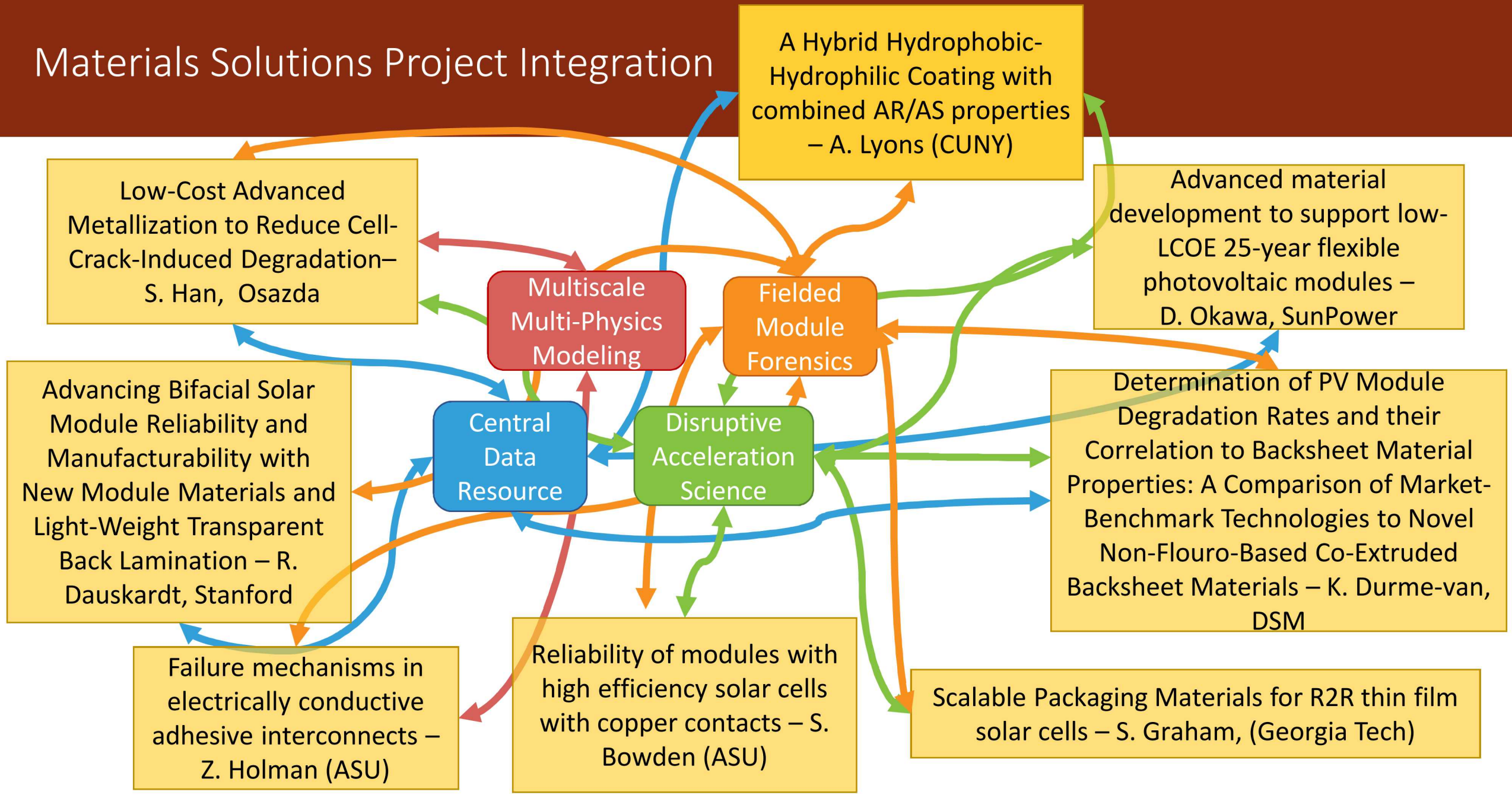

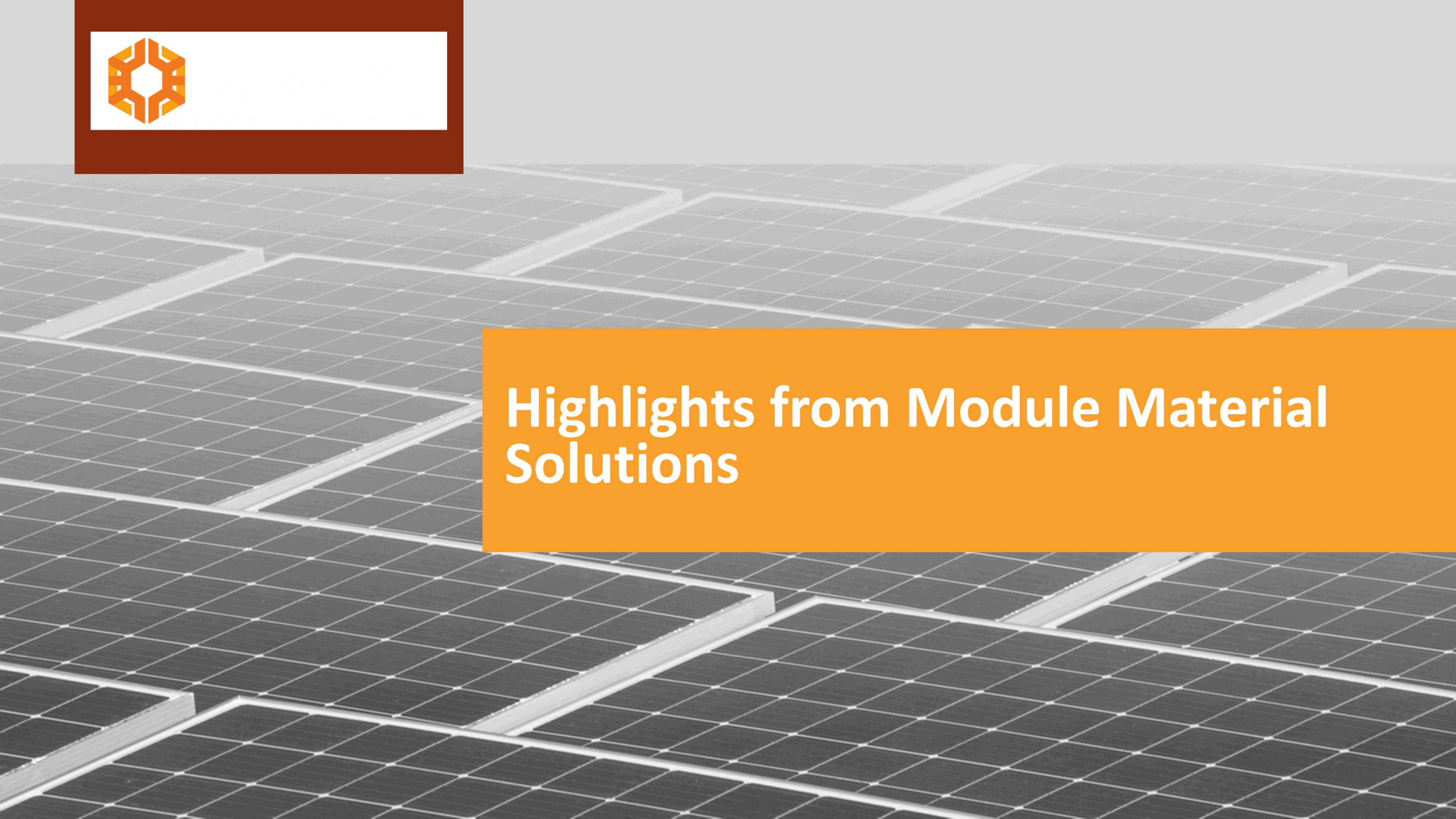

Highlights from Module Material Solutions

Scalable Packaging Materials for Roll-To-Roll Processed Thin Film Solar Cells

PI: Samuel Graham/Georgia Institute of Technology

Technology Summary and Impact

- Enable flexible packaging for thin film solar through testing barrier and adhesive materials compatible with R2R processing of solar cells for long term stable performance.
- Developed reproducible methods to screen the permeability of the adhesives and to characterize the strain energy release rate of the interface.
- For perovskite cell packaging:
  - Desiccant filled systems are necessary to maintain low permeation properties while systems like EVA and polyolefins provide the highest initial adhesive strengths. In addition, barrier layer containing 3M UBF is necessary as it provides superior UV stability amongst the flexible substrates.

Barrier Film and Adhesive Development

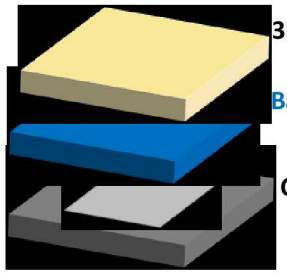

High Throughput Testing

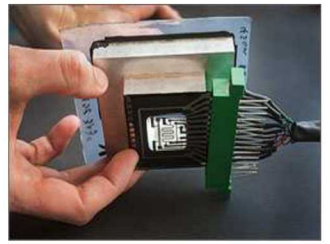

Integration with Thin Film PV

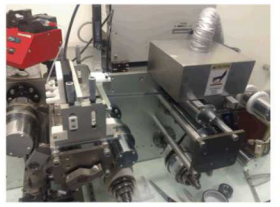

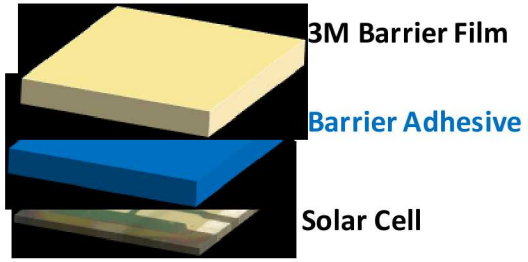

Teaming

Team: Samuel Graham, CP Wong, Suresh Sitaraman (Georgia Tech), Matthew Reese (NREL)

Accelerated UV Aging of Encapsulants and Edge Sealants

Sample Fabrication

- **In-house** fabricated PET/EVA/PET and 3M UBF/EVA/3M UBF sandwich using hot press
- PET/EVA/PET and 3M UBF/EVA/3M UBF sandwich fabricated at **NREL** using vacuum laminator (PET and 3M UBF were **also corona treated** to enhance the adhesion)

Vacuum Laminator (NREL)

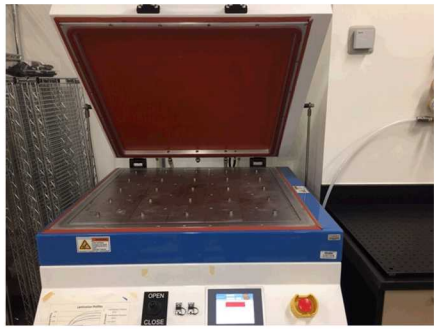

Corona Treatment Set-up (NREL)

Peel Testing

- More compatible with flexible materials
- High-throughput

Testresources.net

Peel Testing Parameters

- Displacement control at 100mm/min
- 250 lbs., 25 lbs., or 2.2 lbs. load cell

Aging Study

- UV: 365nm @ 831 W/m^2 (Dosage: 18 Sun) – generates temperature up to 65 °C.

Initial Peel Strength of Encapsulants (with and without Corona Treatment, CT)

STR EVA/PET	STR EVA/3M UBF	STR EVA/CT PET	STR EVA/CT 3M UBF
1.01 ± 0.09 N/mm	1.75 ± 0.45 N/mm	6.25 ± 0.85 N/mm	6.08 ± 0.64 N/mm

In-House Fabricated Samples

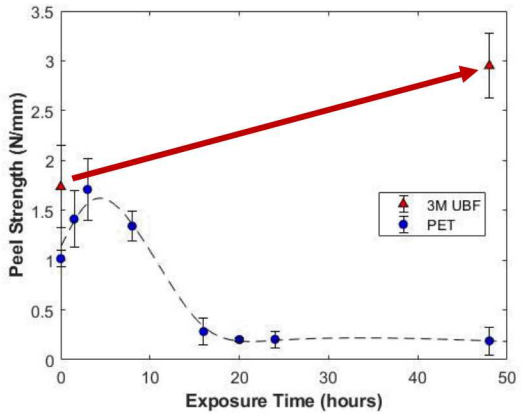

Lamination: Hot-Press
Surface Treatment: None

Samples Fabricated at NREL

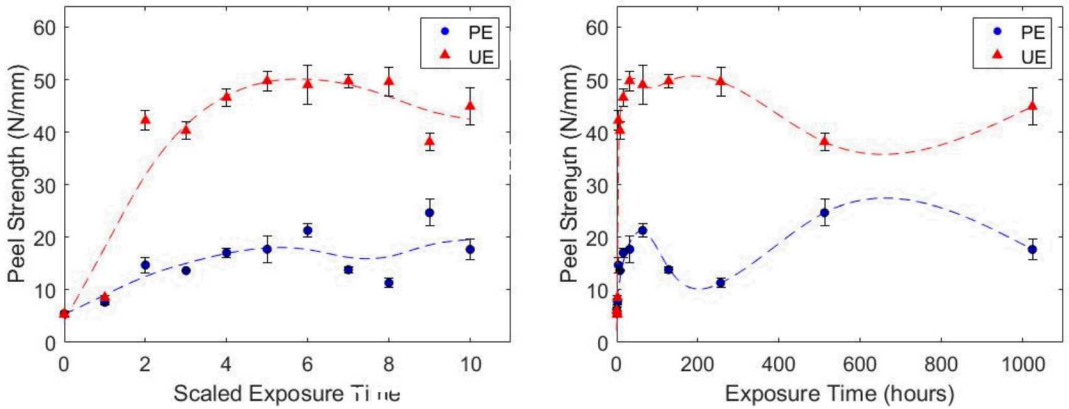

Lamination: Vacuum Laminator
Surface Treatment: Corona Treatment (CT)

- UV exposure initially increases PET/EVA (PE) and 3M UBF/EVA (UE) adhesion strength.
- Adhesion strength of the samples fabricated at NREL (different fabrication processes) increases their adhesion strength up to ~20X (in combination of both corona treatment +and UV/thermal aging effect).
- Prolonged UV exposure degrades the PET/EVA interface (photo-induced polymerization vs photo-induced oxidation).
- Samples of t_{512} for PE does not follow the earlier trend (does t-peel really tell about the interface, and what if crosslinking density increase from UV irradiation causes embrittlement and requires higher load to peel the sample?)
- UE samples, however, are more resilient towards the UV-thermal aging from mechanical T-Peel perspective.

Failure Mode for T_{1024} Sample for PET/EVA

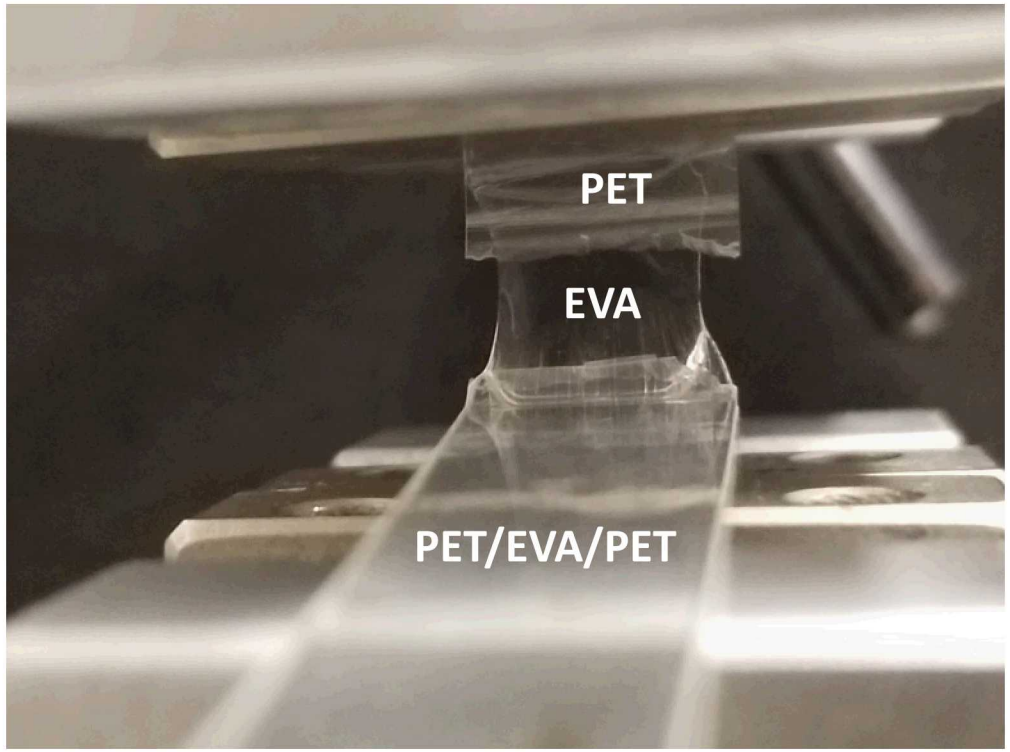

Figure 4. Failure Mode of the PET/EVA interface upon 1024 hours of UV exposure.

Toughness of the PET is weaker than that of the EVA.

Damage on the actual protective backsheet is more severe than on the EVA.

FTIR Characterization on the EVA Side of the Delaminated Samples

Motivation

To understand the UV-thermal aging influences from photo-oxidation on the surface of EVA (bulk characterization; depth of penetration: few microns)

Table I. Carbonyl Index (CI) of delaminated EVA from different protective polymer backsheet for varying UV aging time from FTIR Characterization.

Sample	Aging Time (hr)	A_{1780}/A_{2850} *Lactone Carbonyl Formation*	A_{1735}/A_{2850} *Ester Carbonyl Stretching*	A_{1715}/A_{2850} *Ketone Carbonyl Stretching*	A_{1175}/A_{2850} *Ketone Carbonyl Stretching*	A_{1163}/A_{2850} *Aliphatic Ester*
ST505 PET/ EVA	0	0.024	0.630	0.082	0.044	0.042
	32	0.022	0.630	0.079	0.041	0.038
	256	0.023	0.620	0.080	0.044	0.043
	512	0.023	0.617	0.079	0.043	0.041
	1024	0.023	0.645	0.080	0.039	0.036
3M UBF/ EVA	0	0.025	0.630	0.075	0.040	0.036
	32	0.025	0.622	0.076	0.039	0.036
	256	0.024	0.618	0.076	0.039	0.036
	512	0.025	0.615	0.075	0.039	0.036
	1024	0.023	0.614	0.074	0.038	0.035

*5 different measurements per condition, and all error bars are less than 5%.

- Variation in PET/EVA is more obviously seen than in 3M UBF/EVA as can be seen from A_{1735}/A_{2850}, ester carbonyl stretching peak: 0.630 → 0.645 for PET/EVA and 0.630 → 0.614 for 3M UBF/EVA. Formation of ester is one of the indications for UV degradation on the EVA film.
- No lactone formation from back-biting process in the vinyl acetate (VAc) units by the acetate group was observed for both samples.
- In general, the normalized absorbance values are too insensitive to determine both from visually from the graph and quantitative analysis.
- It is probable that EVA damage is not too critical due to the presence of Benzotriazole (UV Absorber) and Hindered Amine Light Stabilizer, HALS (UV Stabilizer). Damage on the actual protective backsheet, PET, is more severe (illustrated in next slide).

[1]Allen et. al. *Polymer Degradation and Stability,* **1994**. 43(2): 229 – 237.
[2]Copuroglu et. al. *Polymers for Advanced Technologies,* **2004**. 15(7): 393 – 399.
[3]Copuroglu et. al. *Polymers for Advanced Technologies,* **2005**. 16(1): 61 – 66.
[4]Agroui et. al. *Renewable Energy,* **2012**. 43(1): 218 – 223.

It is noted that a residual amount of the peroxide curing agent will remain in the EVA material after curing.[4]

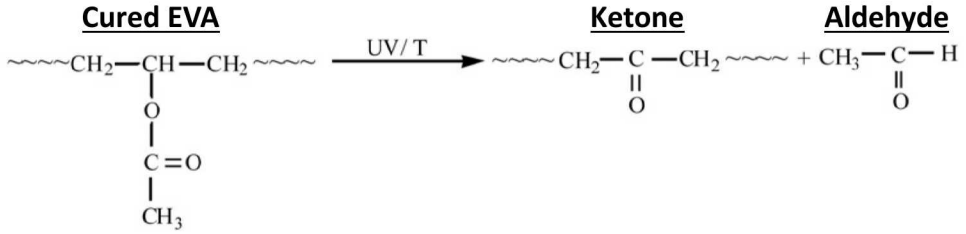

Figure 1. Ketone formation via acetaldehyde evolution (Norrish Type III photolysis reaction).[1]

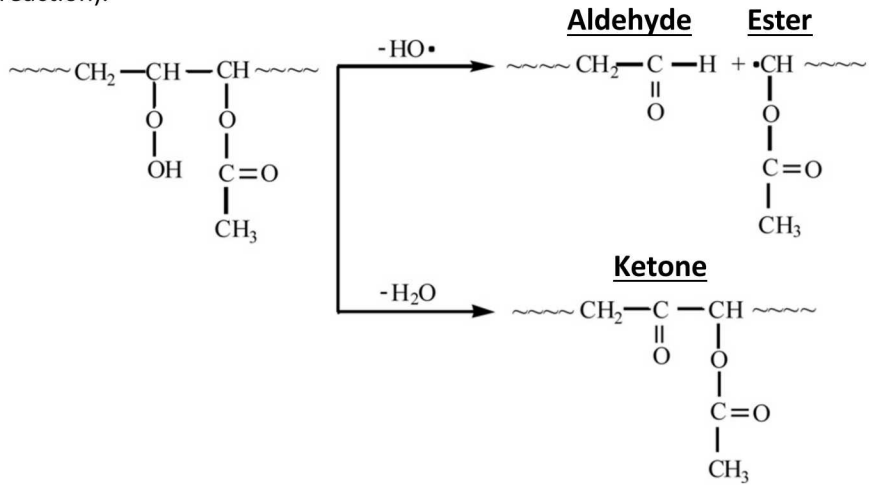

Figure 2. Ketone formation via hydroxide breaking down (water deprivation reaction of the hydroperoxide).[2, 3]

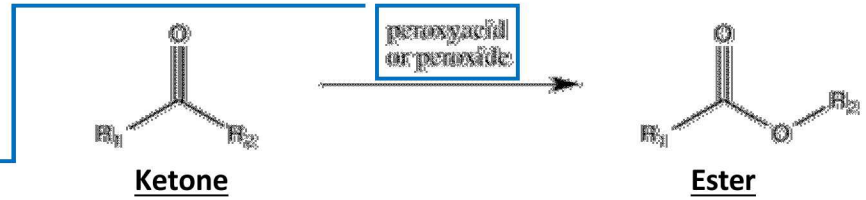

Figure 3. Baeyer-Villiger oxidation reaction.

XPS Characterization of the EVA Side of the Delaminated Samples

Motivation

To understand the UV-thermal aging influences on the interfacial adhesion of EVA/Backsheet material (surface characterization; depth of penetration: few nanometers)

Table II. Average Elemental Composition from Survey Spectra of Delaminated STR EVA Surfaces of **PET/EVA** Interface upon UV Aging at 831 W/m^2 at 365 nm.

		t_0	t_{32}	t_{256}	t_{512}	t_{1024}
Element (%)	C 1s	81.16 ± 0.56	80.79 ± 0.44	81.15 ± 0.51	81.53 ± 1.84	81.54 ± 1.08
	O 1s	14.53 ± 0.35	14.87 ± 0.30	14.99 ± 0.34	14.81 ± 1.50	14.70 ± 0.66
	Si 2p	4.31 ± 0.27	4.34 ± 0.16	3.85 ± 0.28	3.66 ± 0.36	3.76 ± 0.47
O/C Ratio		0.18	0.18	0.18	0.18	0.18

Table III. Average Elemental Composition from Survey Spectra of Delaminated STR EVA Surfaces of **3M UBF/EVA** Interface upon UV Aging at 831 W/m^2 at 365 nm.

		t_0	t_{32}	t_{256}	t_{512}	t_{1024}
Element (%)	C 1s	82.84 ± 0.45	85.59 ± 0.43	84.64 ± 0.47	84.96 ± 1.43	84.93 ± 0.81
	O 1s	12.78 ± 0.15	11.13 ± 0.14	12.18 ± 0.13	11.73 ± 0.83	12.11 ± 0.41
	Si 2p	4.38 ± 0.35	3.28 ± 0.32	3.18 ± 0.59	3.32 ± 0.62	2.97 ± 0.44
O/C Ratio		0.15	0.13	0.14	0.14	0.14

- EVA surfaces of delaminated PET/EVA sample does not show an abrupt change in atomic concentration of individual element, whereas those of delaminated 3M UBF/EVA sample show an increase in atomic concentration of carbon, thus decrease in atomic concentrations of oxygen and silicon (decrease in the atomic concentration of silicon is more severe for 3M/EVA sample: **cleavage sites of the PET/EVA and 3M UBF/EVA interfaces differ**).
- Due to a higher force required to delaminate the 3M UBF/EVA interface, less amounts of oxygen and silicon atomic concentration was detected on the surface of the delaminated EVA, in which it inversely corresponds well to the mechanical T-Peel test data (**inverse relationship between silicon atomic concentration vs peel strength**). Note that silicon peak detected corresponds to the silane adhesion promoters present on the surface of the EVA.

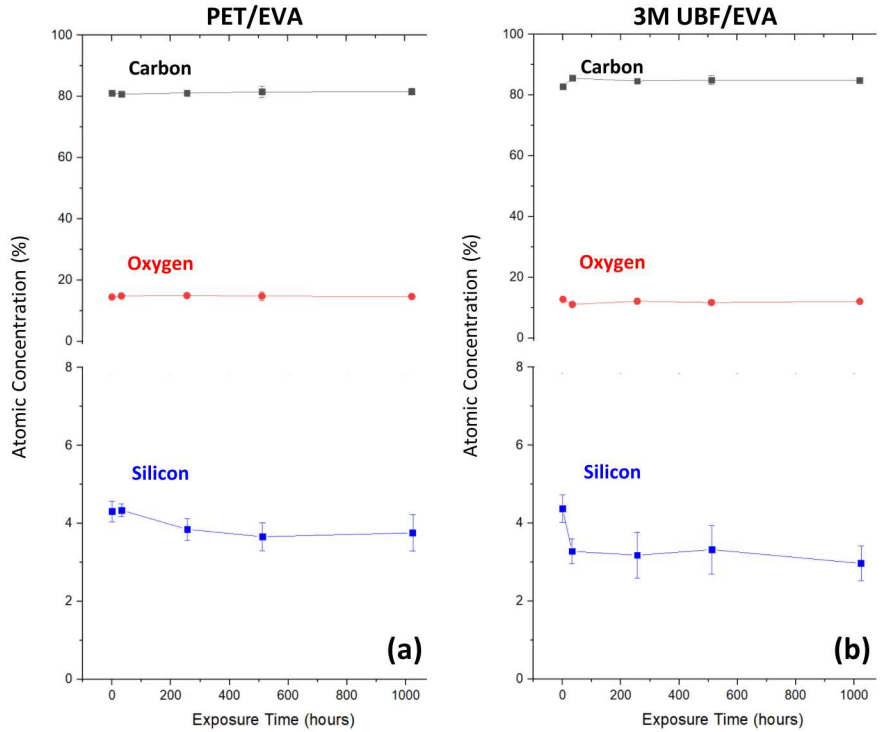

Figure 4. Average elemental composition of delaminated surface of EVA (a) PET/EVA and (b) 3M UBF/EVA

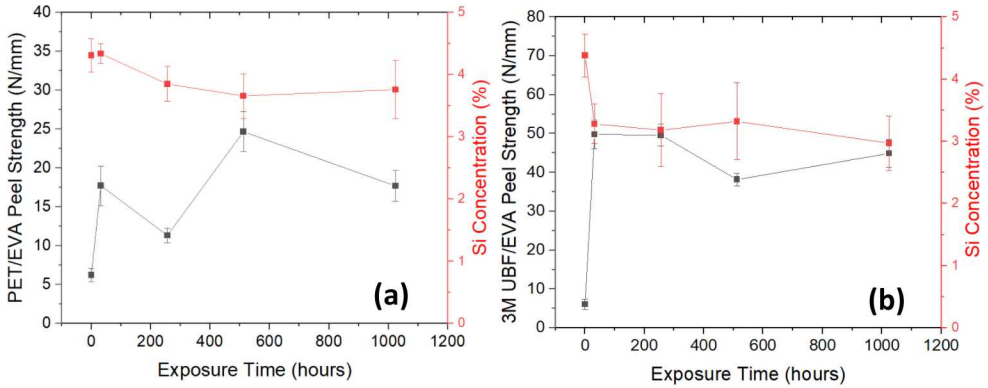

Figure 5. Peel Strength vs Si Concentration of (a) PET/EVA and (b) 3M UBF/EVA.

Perovskite Solar Cell Encapsulation – New Encapsulation Method

Motivation

To design a packaging methodology to successfully stabilize the environment-sensitive perovskite solar cells.

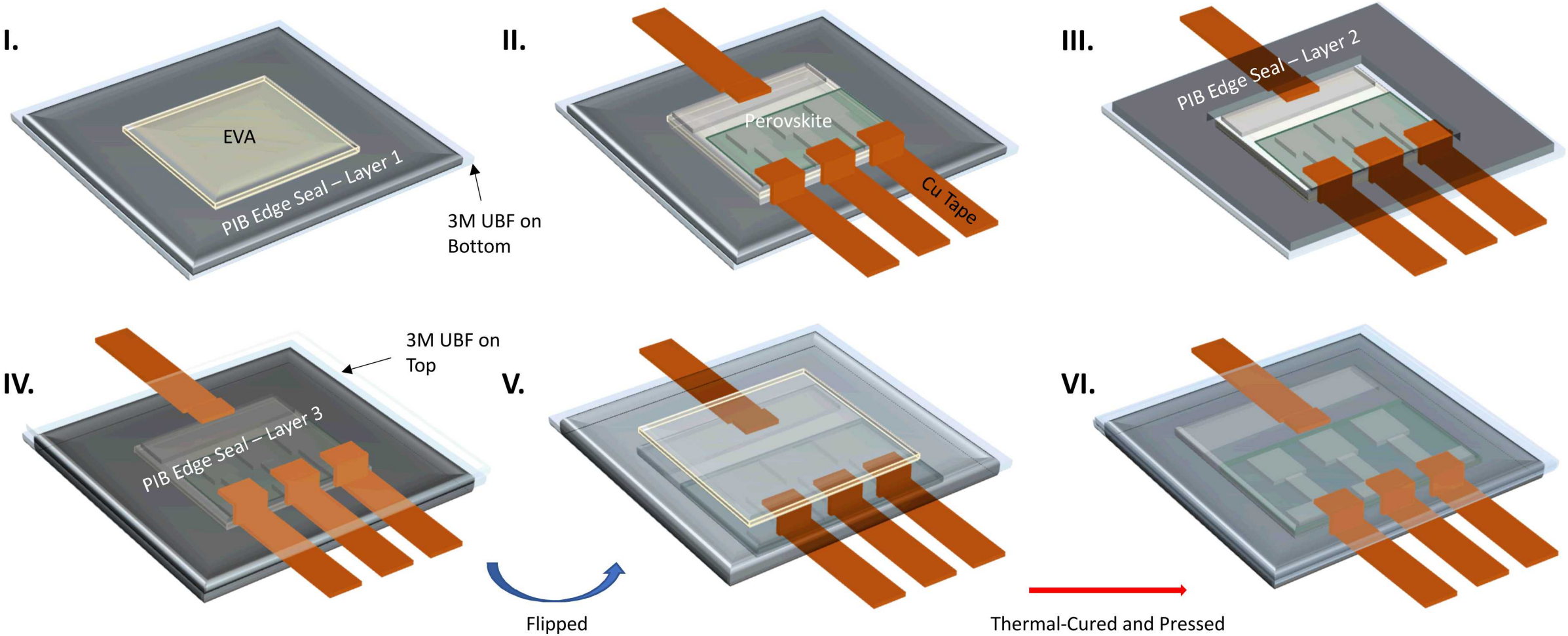

Figure 6. Encapsulation process of perovskite solar cell

Stability of the Encapsulated Perovskite Solar Cell

Motivation

To characterize the stability of the environment-sensitive perovskite solar cells.

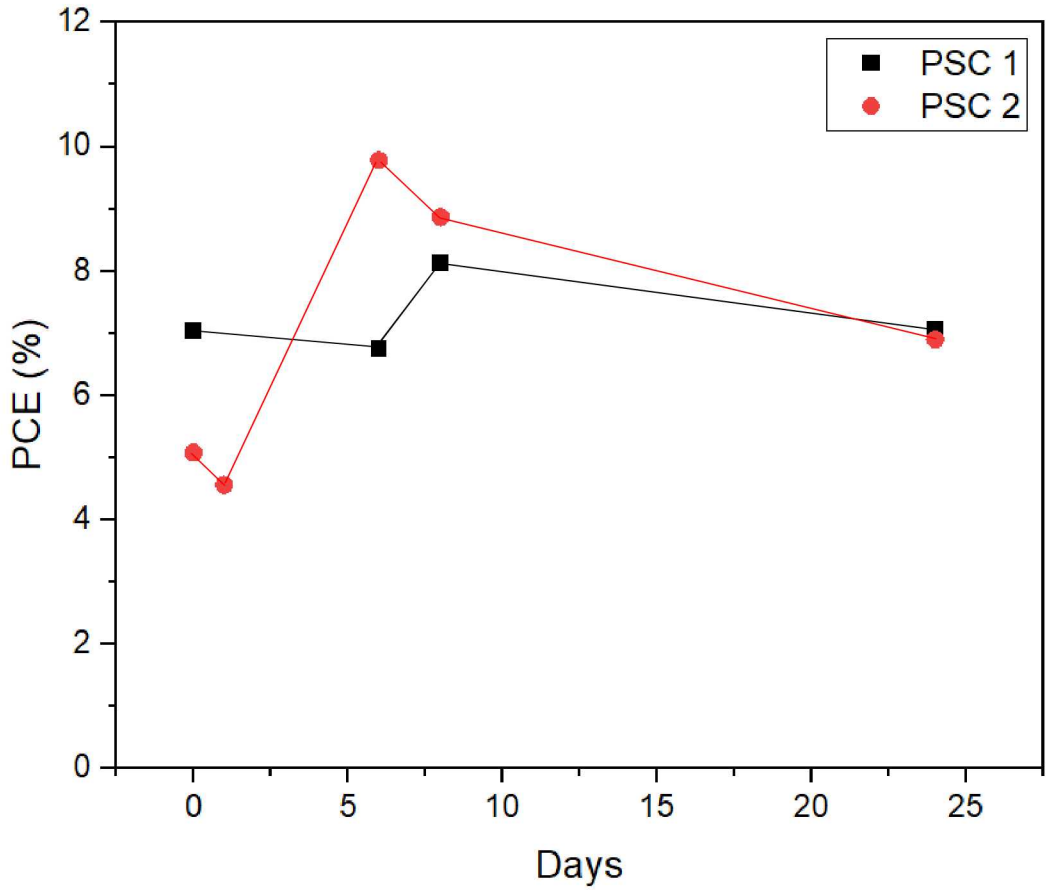

Figure 7. PCE values of the encapsulated perovskite solar cell under room temperature/humidity condition.

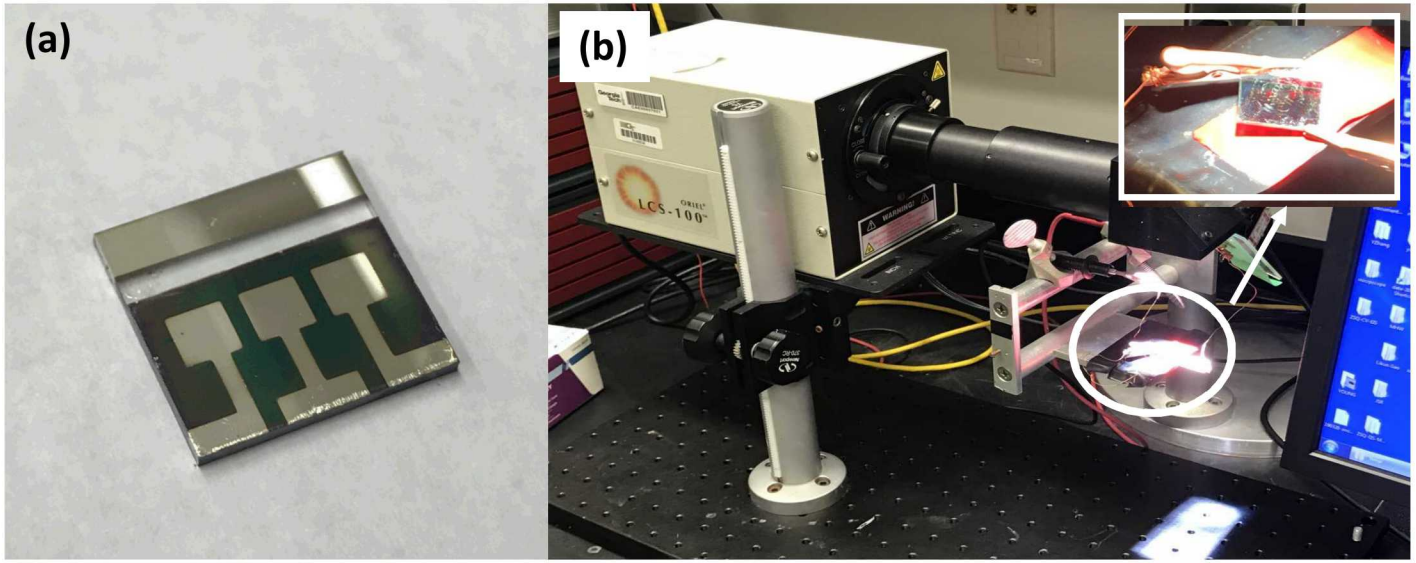

Figure 8. Encapsulation of PSC **(a)** In-house fabricated PSC, in collaboration with wide-bandgap PSC fabrication group at GT, **(b)** PSC efficiency measurements, where inset shows two connections to the Ag electrodes

Sunside

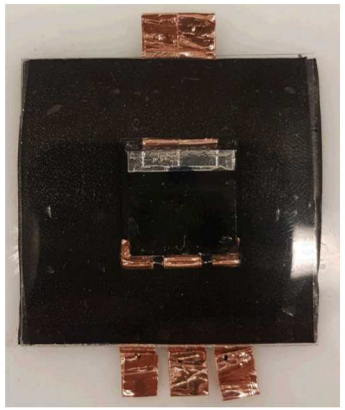

Backside

Hydrophobic-Hydrophilic Coatings for PV Solar Cover Glass
PI: Alan Lyons – City University of New York

Technology Summary and Impact

Durable Module Material

- Robust and low-cost coating on glass providing >3% AR gain and >50% soiling reduction.

Innovation

- Preferential nucleation of liquid water on hydrophilic regions, and the high mobility of droplets on hydrophobic, anti-reflective regions combine to increase water collection rates by a factor of 2 compared to uncoated glass while decreasing reflections.
    - **Impact**: Realizing these properties would achieve up to 91% of the SunShot 2030 O&M cost-reduction goal of 0.7¢/kWh.

Harvest "free" water from dew to self-clean cover glass

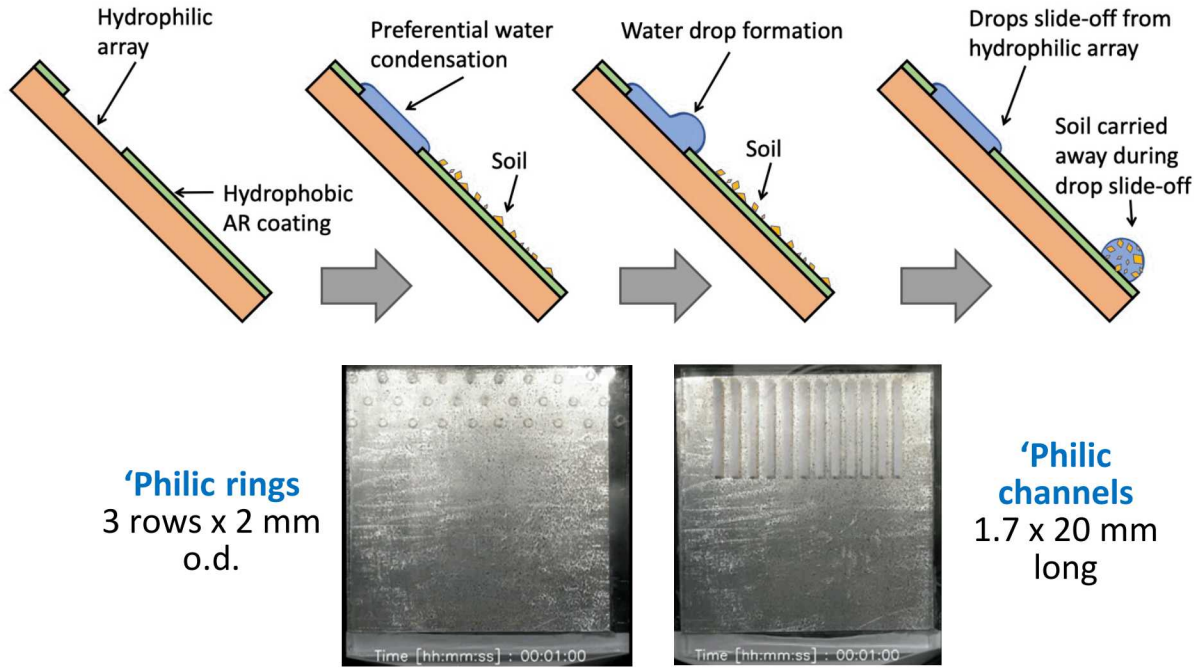

Resources

Journal Articles:

https://doi.org/10.1016/j.solmat.2019.110281

https://ieeexplore.ieee.org/document/8937750

Teaming

Team: Alan Lyons and Illya Nayshevsky – City University of NY; NREL - David Miller and Jimmy Newkirk; ARL Designs LLC - QianFeng Xu; DOE RTC – Bruce King and John Sherwin

Highlight: Publication in Solar Energy Materials and Solar Cells

"Fluoropolymer Coatings for Solar Cover Glass: Anti-Soiling Mechanisms in the Presence of Dew"

Illya Nayshevsky[1], QianFeng Xu, Gil Barahman[2] and Alan Lyons,

[1]PhD candidate in Chemistry at CUNY, [2]Undergrad at CUNY; Published on-line 11/25/2019,https://doi.org/10.1016/j.solmat.2019.110281

Hydrophobic and Superhydrophobic (SH) coated glass exhibit significantly improve performance over hydrophilic surfaces

- **SOILING: Hydrophobic and SH FEP coatings reduce soiling by 42% compared to Hydrophilic coatings and Bare Glass**
  - Condensation mechanism determines soiling rate.
    - Hydrophobic and SH surfaces: condensation occurs via dropwise mechanism. Hemi-spherical drops less than 100 µm diameter
    - Hydrophilic and Bare glass surfaces: condensation occurs via filmwise mechanism. Irregularly shaped puddles 0.2 – 1.1 mm diameter.
  - Surface Roughness not correlated to soiling rate
    - Hydrophobic and hydrophilic coatings have similar roughness (7 vs 11 nm) but different wetting and condensation properties

- **CLEANING: Hydrophobic and SH surfaces clean more effectively than hydrophilic and bare glass**
  - Hydrophobic & SH coatings improve cleaning efficiency both in the presence of dew, as well as on dry surfaces
  - No-touch cleaning (water only) after soiling results in >99.6% of original %T restored on Hydrophobic and SH surfaces

	Bare Glass	Hydrophilic-1	Hydrophobic-1	Superhydrophobic
AFM Images	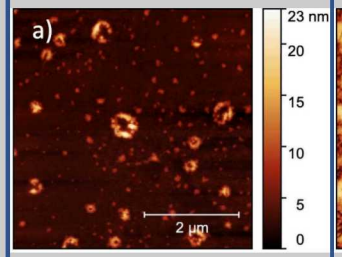	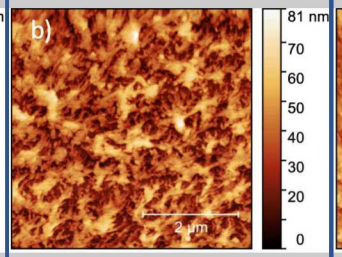	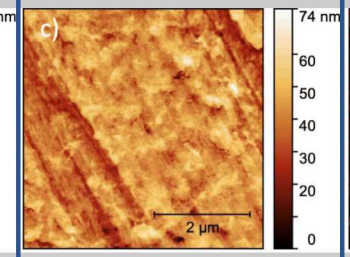	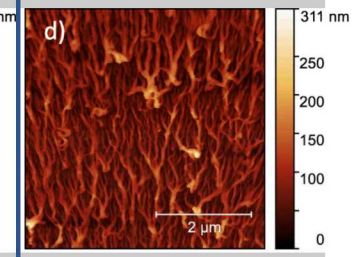
Contact Angle	10°	63°	106°	149°
RMS Roughness	2 nm	11 nm	7 nm	31 nm
Condensation Type	Filmwise	Filmwise	Dropwise	Dropwise
Condensate dia.	1,100 µm	170 µm	50 µm	40 µm
%T change after soiling	-5.7 %	-5.9 %	- 3.5 %	-3.4 %
%T change after cleaning	-4 %	+15 %	+75 %	+90 %

Highlight: Publication in IEEE Journal of Photovoltaics

"Self-cleaning hybrid hydrophobic-hydrophilic surfaces: Durability and effect of artificial soilant particle type"

Illya Nayshevsky[1], QianFeng Xu, James Newkirk[2], Daniel Furhang,[3] David Miller, and Alan Lyons

[1]PhD candidate in Chemistry at CUNY, [2]Undergrad &intern at NREL, [3]Undergrad at CUNY

Published on-line 12/19/2019, DOI: 10.1109/JPHOTOV.2019.2955559

Durability of Hydrophobic Coating: Artificial Weathering

No significant change to FEP surface after 2000 h (7.2 MJ m^{-2})

- IEC TS 62788-7-2 A3 method
- Irradiance: 0.8 $W \cdot m^{-2} \cdot nm^{-1}$ at 340 nm
- Chamber: 65°C, 20% RH, black panel: 90°C.

Representative Solar Weighted Transmittance (RSWT)

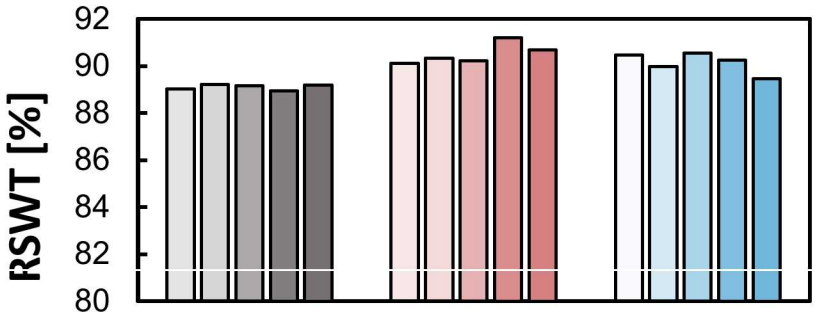

Contact Angle after UV Exposure

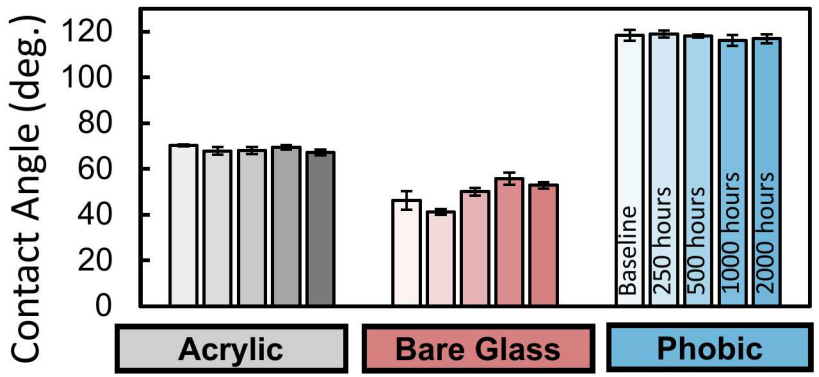

Effect of Soil Type and Tilt Angle on Anti-Soiling & Self-Cleaning Performance

- **Hydrophobic FEP coated glass reduces soiling by 46% compared to Bare Glass**
  - Insoluble and unreactive soils (AZ test dust and Aramco) soil more slowly compared to minerals that react with water ($CaCO_3$ and Portland cement), which reduce %T more.
- **Hydrophobic and Hybrid coated glass exhibit self-cleaning properties under simulated dew**
  - Bare Glass is NOT cleaned by condensation alone.
  - Hydrophilic rectangular channels improve self-cleaning properties
  - Droplets slide off Hybrid surface ~10% sooner than Phobic Surface
  - Droplets on Hybrid surface are larger, cleaning larger swath

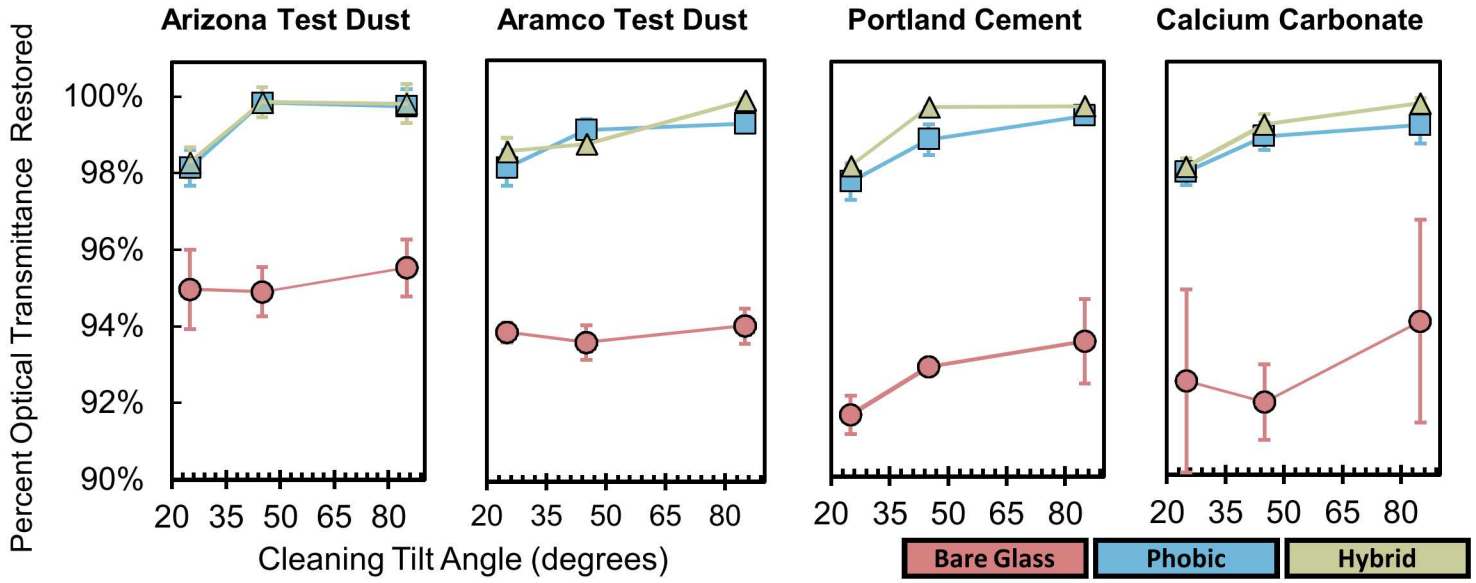

Failure mechanisms in electrically conductive adhesive interconnects
Arizona State University/QESST, Zachary Holman

Technology Summary and Impact

- Establish models for ECA interconnect failure mechanisms
- design accelerated tests in accordance with those mechanisms
- evaluate select commercial ECA interconnects using those tests.

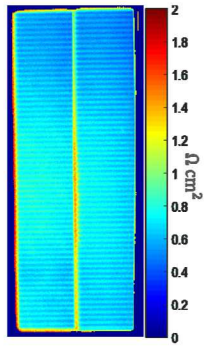

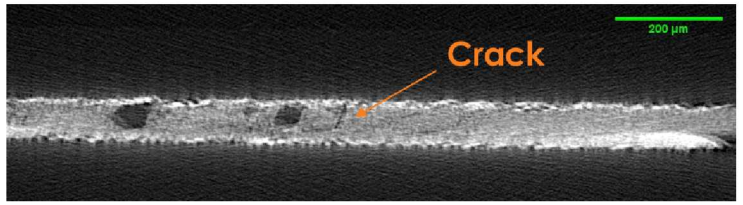

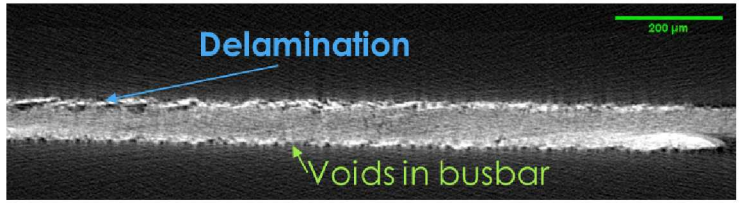

Resources

Collaboration between projects with N. Bosco: Unified Constitutive Model for ECA Degradation

Teaming

Team: Zak Holman, Barry Hartweg, Kate Fisher – ASU
Nick Bosco, Martin Springer – NREL

X-ray computed tomography for 3D particle analysis

Scientific Achievement:

- X-ray computed tomography (XCT) has been confirmed as an accurate measurement technique for ECA metal particle analysis
- XCT measured an average particle diameter equivalent of 4.2 ± 2.9 µm, while SEM measured 3.7 ± 2.9 µm, suggesting they are in reasonable agreement with each other
- XCT measured a particle volume fraction of 70.4%, while SEM is only able to measure an areal coverage, which was 19.5%

Significance and Impact:

- XCT enables a deeper understanding of the isotropic conduction present in ECAs. SEM alone only analyzes a single plane of the ECA material, which can erroneously suggest that there are minimal viable conduction pathways.
- This analysis will be particularly useful to study the volume fraction through damp-heat testing to determine if adhesive water absorption and swelling is a potential failure mechanism for ECAs.

Research Details:

- XCT and SEM analyses were completed on the same silicone-based ECA sample
- SEM image analysis was completed using thresholding in ImageJ
- XCT data analysis was completed using thresholding in Avizo, which is a 3D image analysis software package

XCT

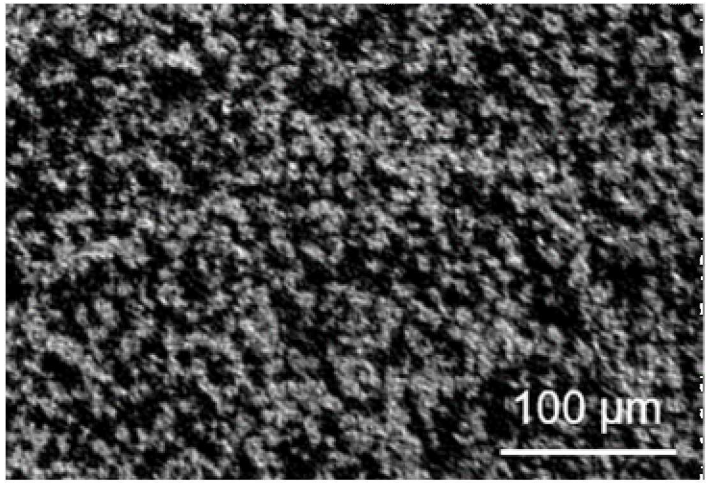

SEM

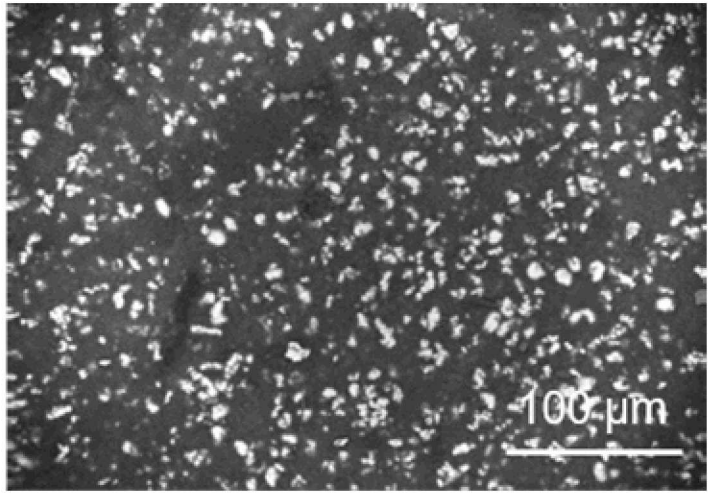

Testing and Model Progress

- Bulk resistivity and contact resistivity reliability experiments were completed.

- Shingled modules and bare ECA test structures were fabricated.
- Aging in DH and dry was completed.
  - Some failures were observed and initial analysis was completed with a few leading hypotheses as to the cause of the failures. More analysis to be completed beyond the project end with the intent to publish the final results.

- The model is now being developed in a sister project lead by PI Bosco at NREL
  - Comparisons with FEA model will be completed for future publication.

- In process: manuscript for journal publication.

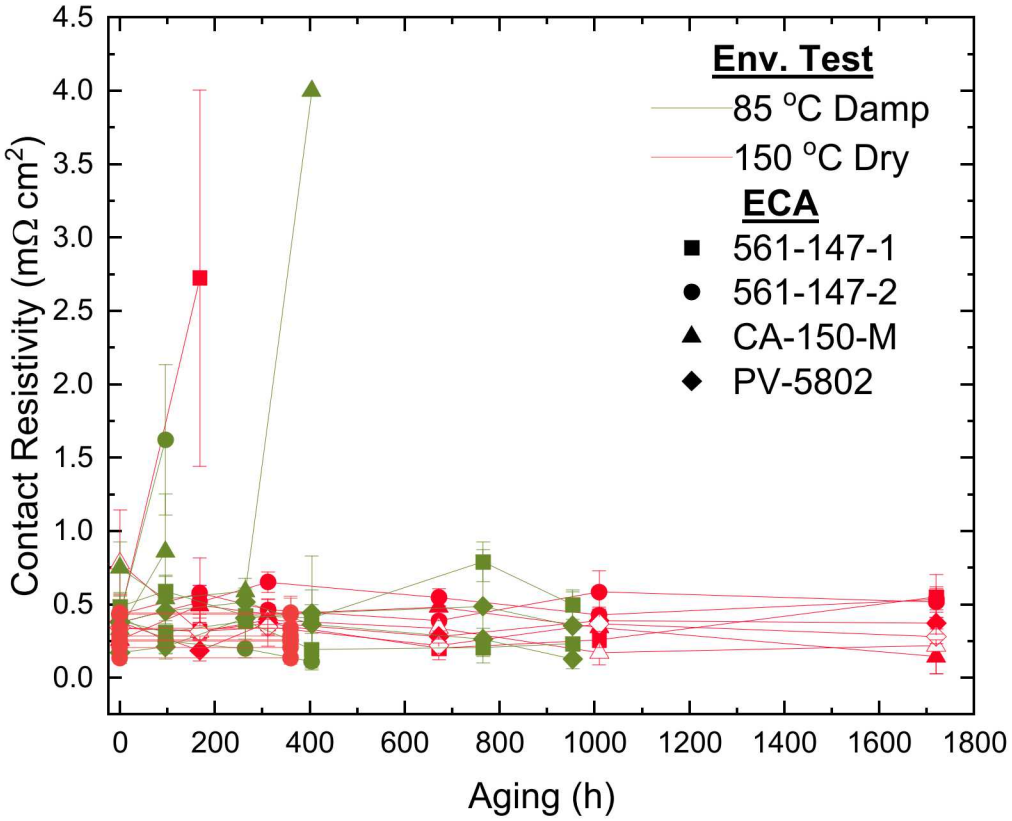

Reliability of Modules with High-efficiency Solar Cells with Copper Plated Contacts

PI: Stuart Bowden – Arizona State University

Technology Summary and Impact

- **There are limited studies on Cu-plated modules reliability. We are evaluating Cu-plated module reliability by:**
  - ➢Testing modules with different encapsulants using the IEC61215 testing protocol and beyond IEC61215 to observe failure mechanisms in Cu-plated modules
    - Cu diffusion after 2000 hrs DH
    - POE *vs* EVA: acetic acid in EVA leads to SnO formation

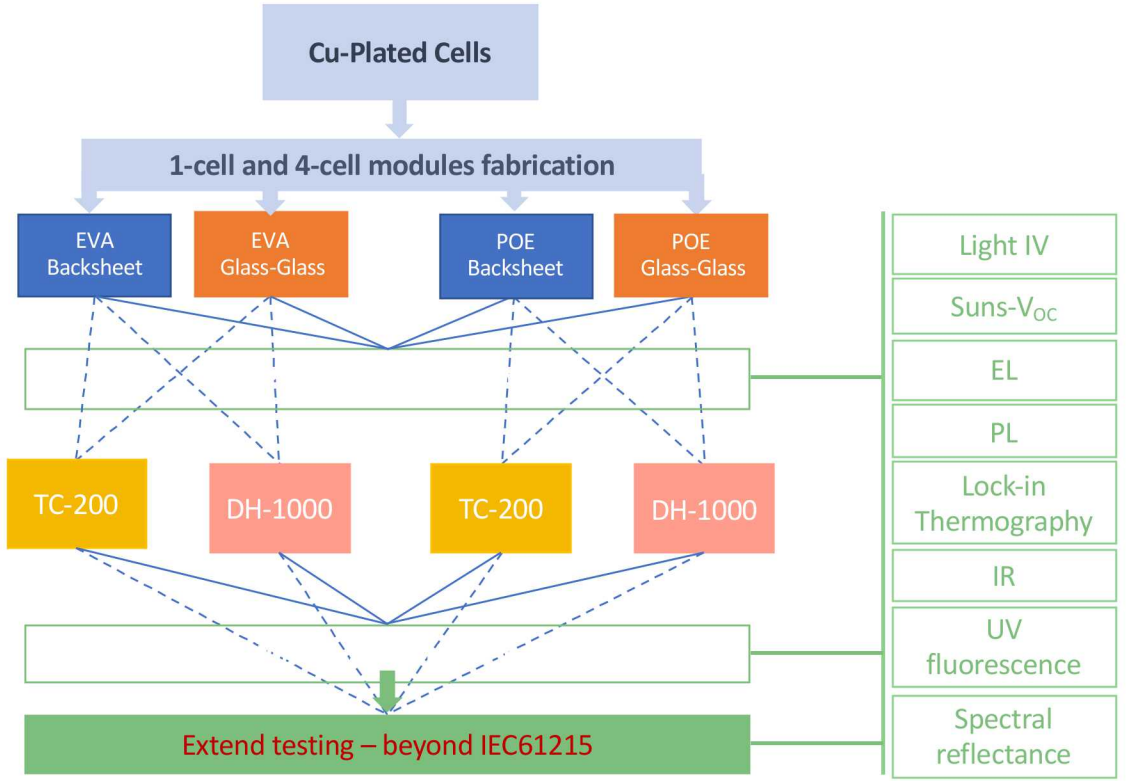

Resources

"Degradation of copper-plated silicon solar cells with damp heat stress." https://doi.org/10.1002/pip.3331

Teaming

Team: Stuart Bowden, Mani TamizhMani, André Augusto, Joseph Karas, Fang Li

Characterization of degraded plated Cu contacts

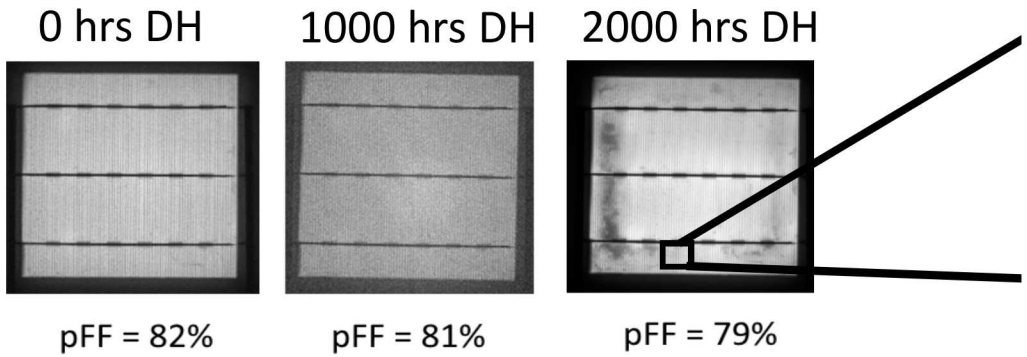

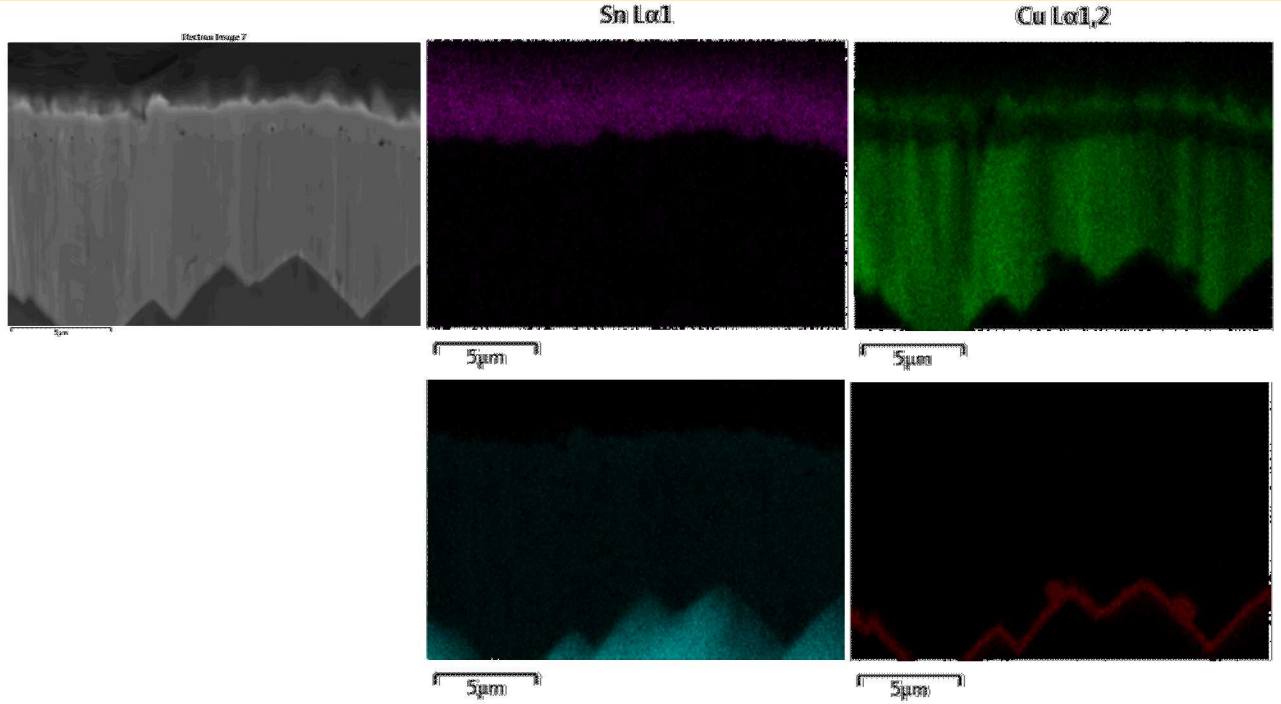

- In collaboration with UNSW (Australia), examined contacts from degraded Cu-plated cells
- Recently-submitted publication details electrical degradation demonstrating diode degradation in DH: "Degradation of copper-plated silicon solar cells with damp heat stress." https://doi.org/10.1002/pip.3331.
  - ➢ Hypothesis: Cu migration from contact (perhaps aided by encapsulant DH-degradation products), causes diode degradation.

- FIB → SEM/EDX cross-sections of contacts from various parts of variously-degraded samples
- EDX evidence of Cu out-diffusion through capping layers (Sn and Ag); void formation at Cu-capping layer interface.
- Paper in progress: Cu out-diffusion so far observed in many Sn-capped and Ag-capped modules in DH with EVA encapsulant.

Characterization of degraded materials from modules with Cu-plated contacts

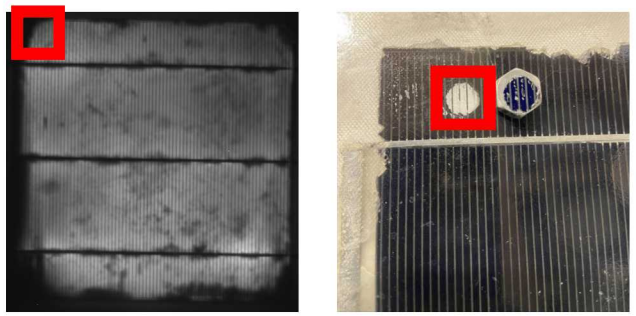

After 4500 hours DH
Cu-plated, EVA-encapsulated

Research goal

- Examine degraded encapsulant and contact surfaces with Raman spectroscopy
- Look for evidence of Cu & Cu corrosion products in EVA
- Determine if DH-degraded EVA plays a role in Cu migration out of contact and/or into cell.

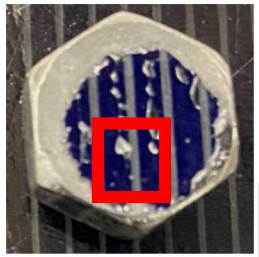

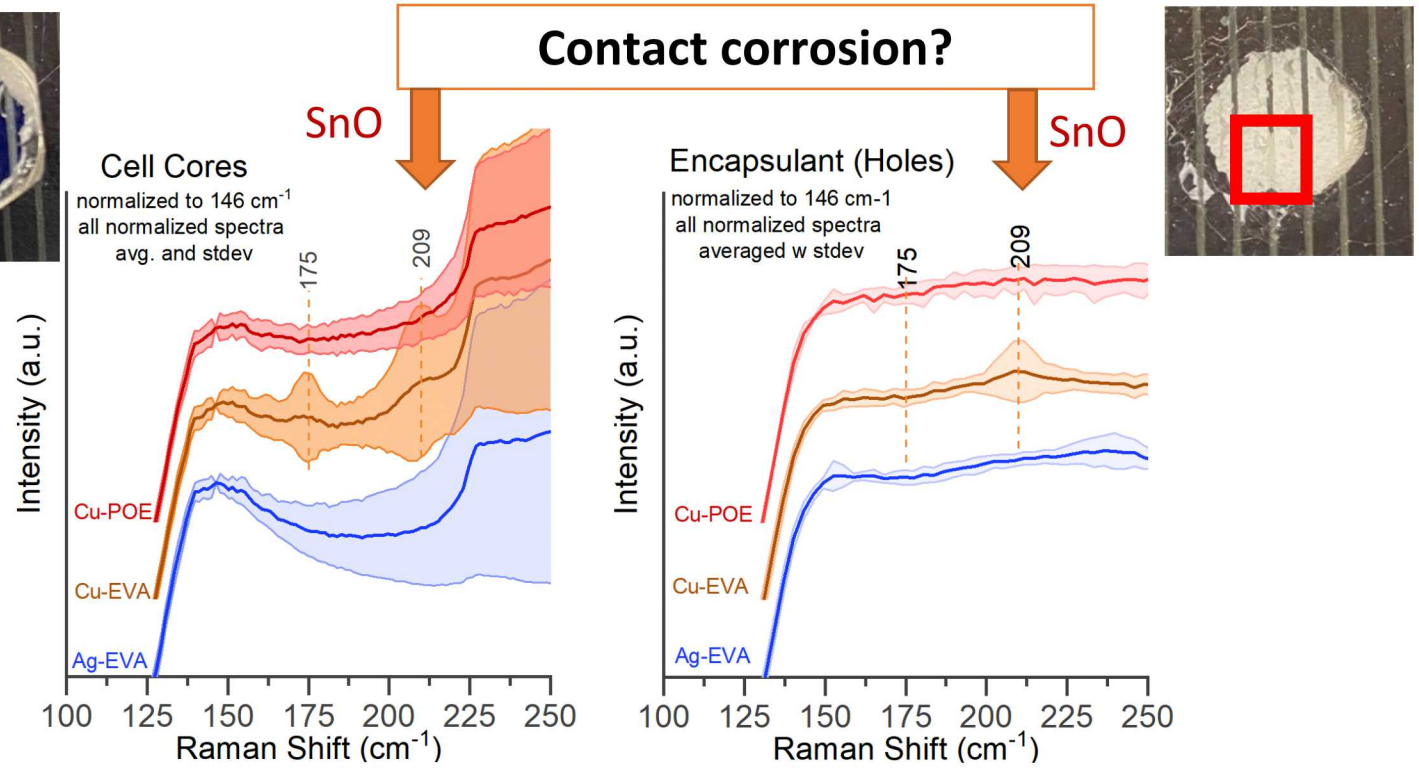

- Contact metal degradation products (SnO) ARE detected on cell and in degraded EVA encapsulant
- Degradation products DO NOT appear in Cu-plated, POE-encapsulated sample, which underwent little degradation
- Sn and Cu are both known to corrode in acetic acid: Cu degradation products might also be present

New Concepts for Reliable Low-Cost Module Encapsulation and Barrier Technologies

PI: Reinhold H. Dauskardt, Stanford University

Technology Summary and Impact

- Thrust 1: Characterize the principal thermomechanical degradation mechanisms relevant to bifacial module materials and interfaces: EVA encapsulation, TPO encapsulation, several heterojunction cell interfaces and metallization lines
- Thrust 2: develop, characterize and validate a transparent polymer backsheet via open-air spray plasma barrier deposition (Stanford), adhesive polymer film formation (DuPont), X-ray characterization (SLAC), moisture content characterization (LLNL), and accelerated testing (Stanford).

Delamination Test

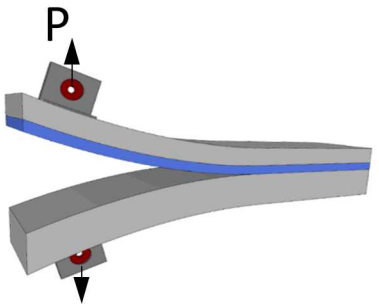

Atmospheric Plasma Deposition

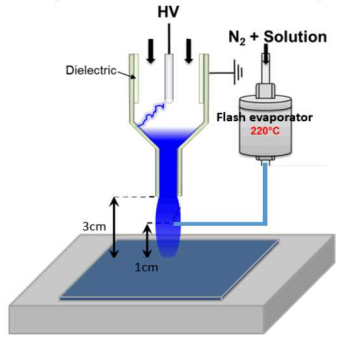

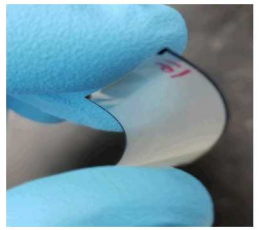

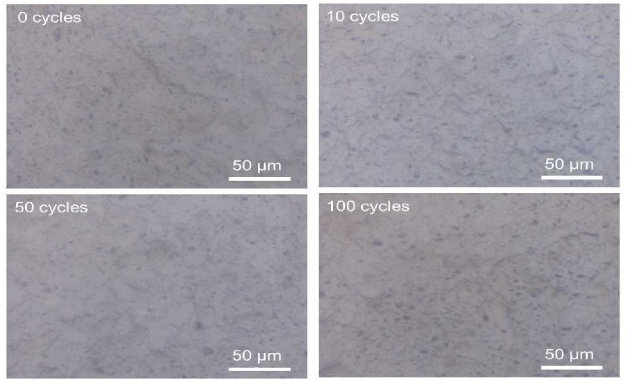

Optical microscope images of barriers deposited onto a flexible polyetherimide (PEI) substrate after bending cycles of a 1.25mm bending radius.

Resources

- P. Thornton, L. Schelhas, S. Moffitt, and R.H. Dauskardt. Fundamental Degradation Mechanisms for Reliability of PV Module Encapsulants, to be submitted to Progress in Photovoltaics.
- O. Zhao, Y. Ding, Z. Pan, N. Rolston, J. Zhang, and R.H. Dauskardt. Open-Air Plasma-Deposited Silica Films in a Multilayer Barrier for Improved Stability of Moisture Sensitive Devices. In review ACS Applied Materials and Interfaces.

Teaming

Team: Stanford University: Oliver Zhao, Patrick Thornton, Ziyi Pan, Reinhold H. Dauskardt

SLAC: Laura T. Schelhas — Solar Tech Universal: Paul Roraff

LLNL: Mihail Bora — DuPont: Drs. Tracy and Kaushik Roy-Choudhury

SAXS and FTIR Characterization of Lab Aged Encapsulant Layers

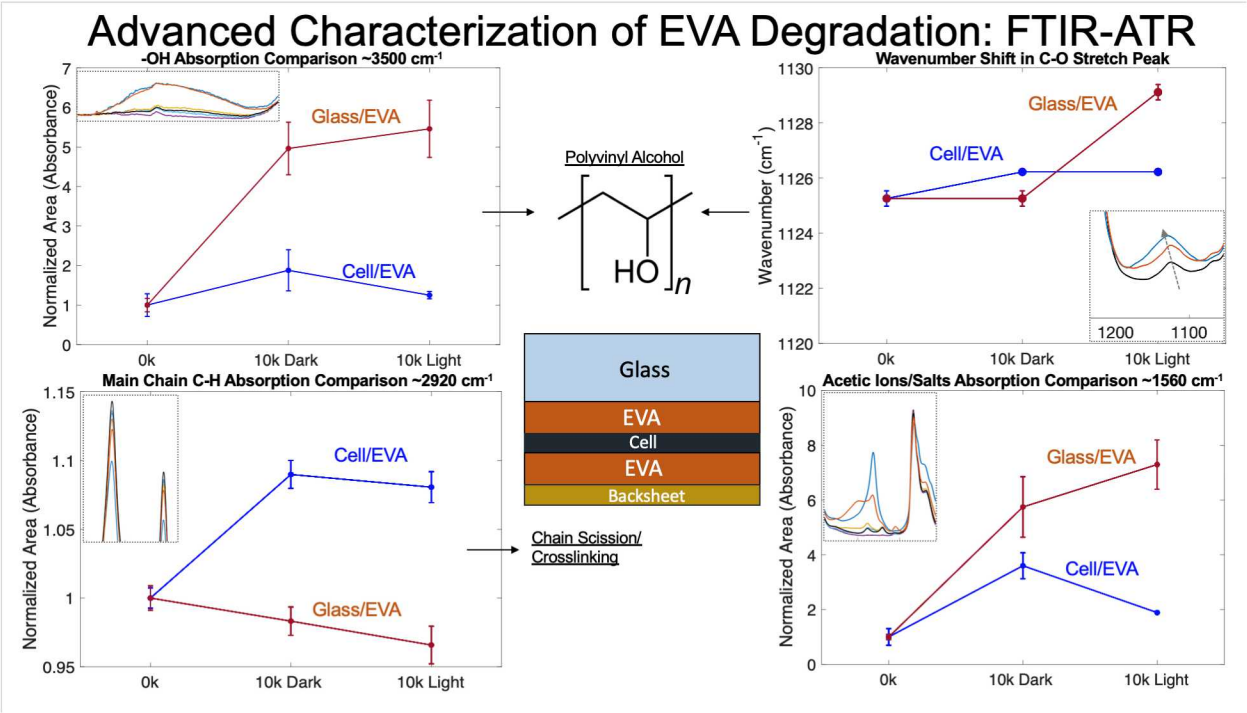

Figure 1 – FTIR-ATR comparisons of the aged EVA at the 2 relevant interfaces).

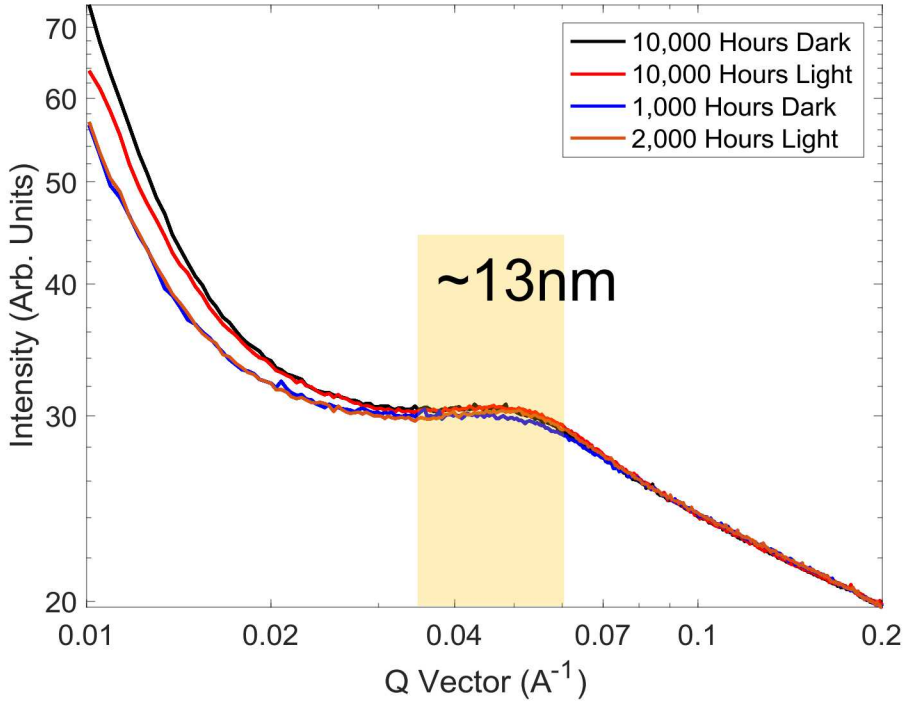

Figure 2 – Transmission SAXS data of various EVA specimen

- FTIR was conducted to investigate the amorphous and crystalline regions. Interfacial results were analyzed and compared (Fig 1) revealing divergent trends at identical aging conditions. After significant analysis and investigation, these data were determined to correlate with an increase in alcohol groups at the glass/EVA interface (Fig 1 – upper 2 plots: signified by the large, broad peak centered around 3400 cm^{-1}) and the presence of significant presence of acetate ions/salts at the glass/EVA interface after long exposure (Fig 1 – lower right plot: the medium sharp peak around 1563 cm^{-1}). Furthermore, data suggests additional crosslinking reactions at the cell/EVA interface with chain scission reactions at the glass/EVA interface (Fig 1 – lower left plot).
- To further analyze the critical size effects in the microstructure of the EVA, SAXS analysis was done. Results indicate an in-plane, characteristic spacing between crystalline and amorphous domains of about 13 nm – a spacing that remains constant over thousands of hours of accelerated aging. Similar in-plane uniformity in aged samples for crystalline lattice structure/spacing was seen in WAXS results previously reported.

In-situ deposited and mechanically robust multilayer barrier

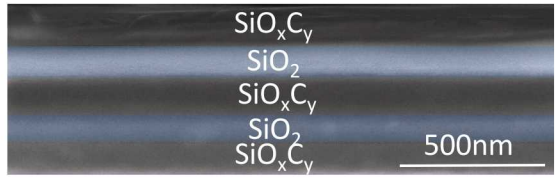

False color SEM image of a five-layer barrier with alternating organic and inorganic layers.

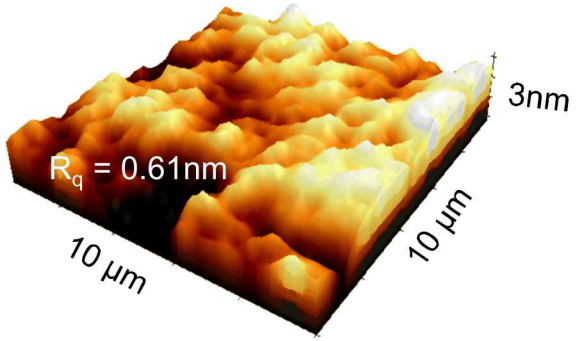

AFM image of SiO_2 layer, showing an extremely smooth surface.

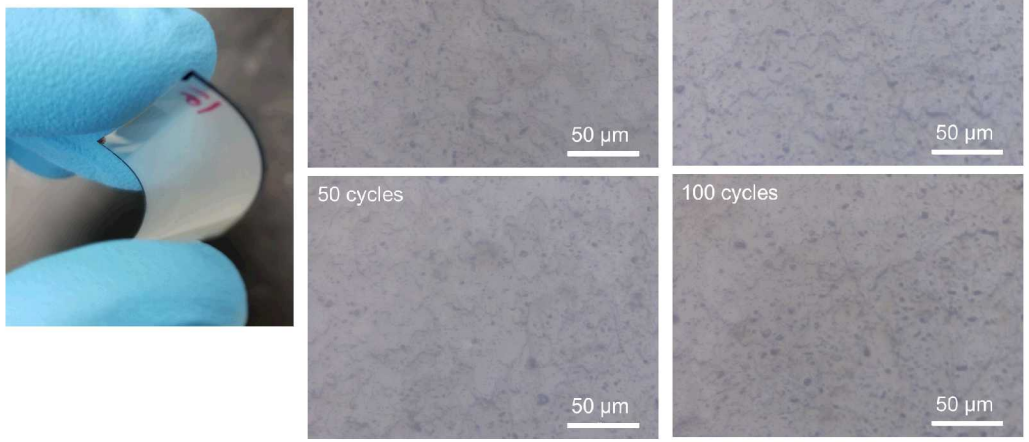

Optical microscope images of barriers deposited onto a flexible polyetherimide (PEI) substrate after bending cycles of a 1.25mm bending radius.

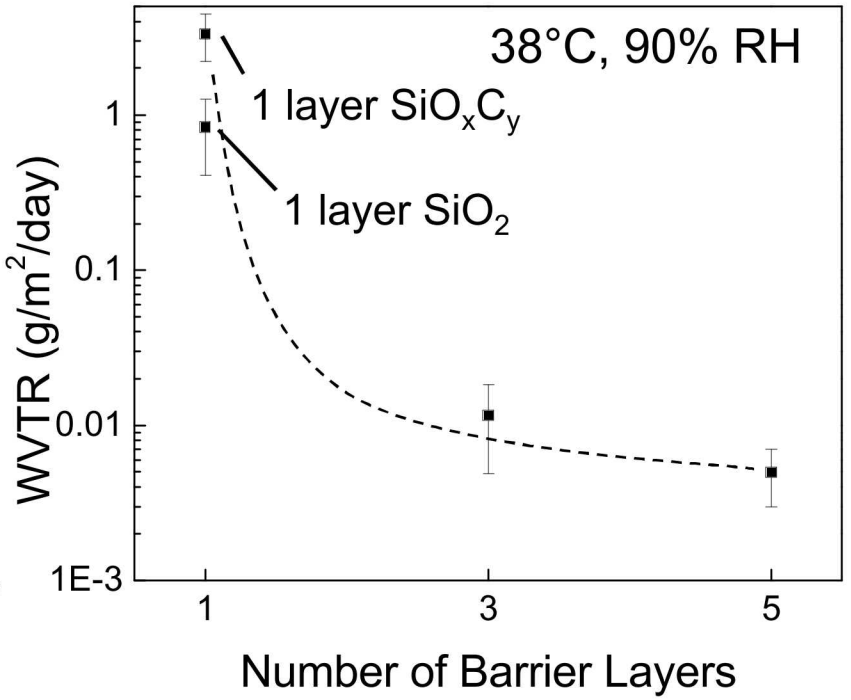

- Thin film moisture barriers deposited in open air offer a potential low-cost solution for module encapsulation without lamination or heat treatment.
- A multilayer design involving alternating layers of inorganic and organic layers leads to synergistic effects between these two layers: the inorganic layer is the effective barrier to moisture or oxygen and the organic layer smooths out roughness on the substrate and passivates possible defects in the inorganic layer.
- The barrier has been successfully deposited onto large area substrates, as well flexible plastic substrates.
- The multilayer barriers on flexible substrates were subjected to bending cycles, where the barrier film was put into compressive and then tensile loading with a 1.25mm bending radius. After 100 bending cycles, there is no visual evidence of cracking in the samples indicating the robust nature of our barrier.
- As shown previously, WVTR was measured using optical calcium testing. Both single layer barriers exhibited WVTR on the order of 0.8 – 4 $g/m^2/day$. However, by combining the layers, there is a significant improvement of WVTR to $1.1*10^{-3}$ $g/m^2/day$. Further improvement to $5.2*10^{-3}$ $g/m^2/day$ was accomplished by depositing a 5-layer barrier.

Development of Bifacial Mini-Modules for Accelerated Testing

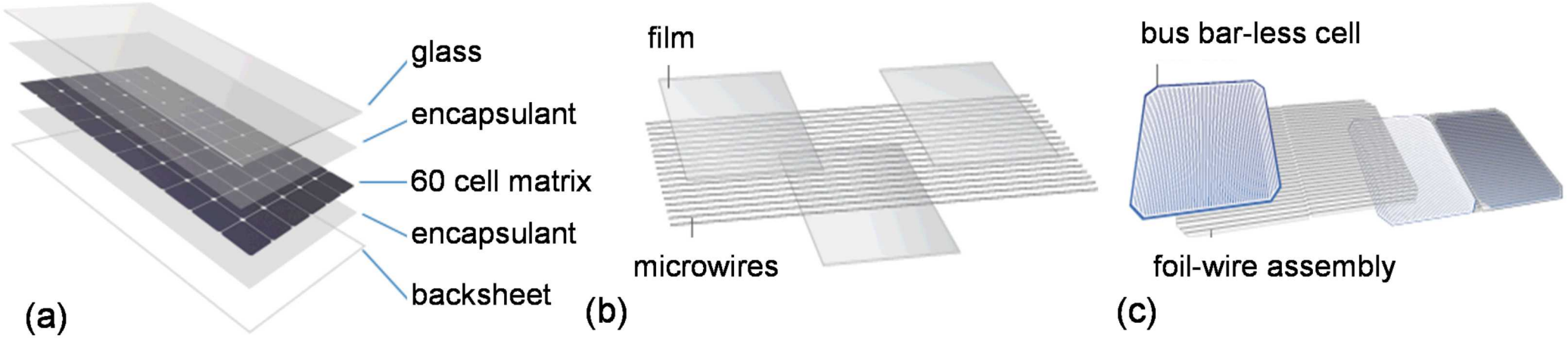

Figure 1 - Key elements of the standard SolarTech Universal module assembly showing key module components and materials including a) layered assembly, b) wire assembly, and c) cell integration.

- Bifacial mini-modules, capable of undergoing accelerated testing and mechanical/chemical characterization at Stanford, are currently in the process of being manufactured and assembled through our partnerships and collaborations with SolarTech Universal and Dupont. SolarTech's module assembly (see Figure 1) will be combined with Dupont's clear fluoropolymer backsheet before Stanford's barrier coating is applied.

Understanding the Role of Trapped Water in Thin Film Barriers

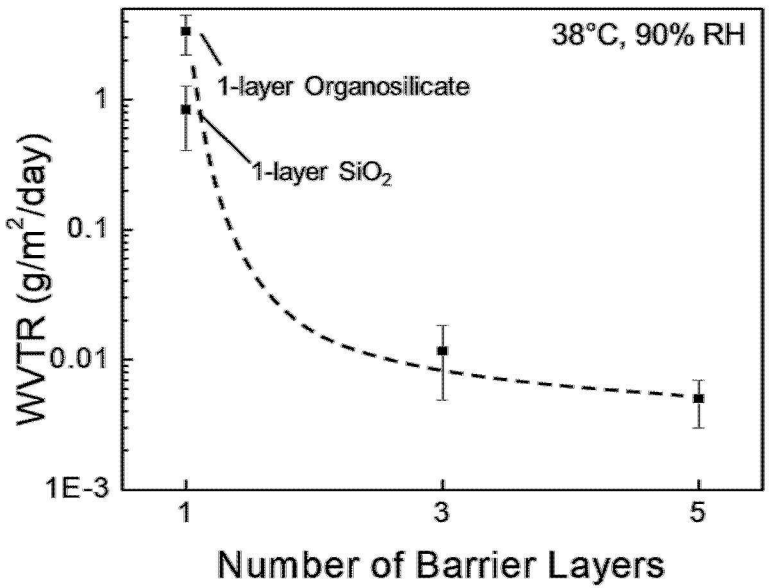

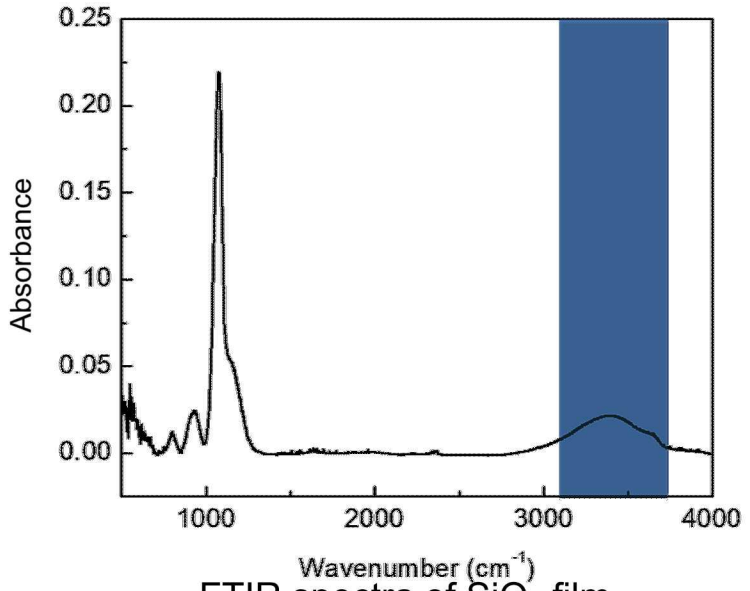

FTIR spectra of SiO_2 film

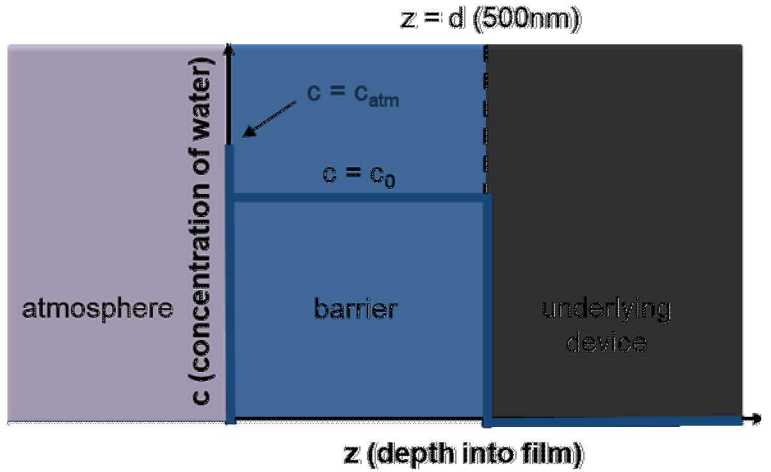

Initial concentration profile

- WVTR was measured using optical calcium testing in accelerated aging conditions of 38C and 90% RH. Both single layer barriers exhibited WVTR on the order of 0.8 – 4 g/m^2/day. By combining the layers, there is a significant improvement of WVTR to 1.1*10^{-3} g/m^2/day. Further improvement to 5.2*10^{-3} g/m^2/day was accomplished by depositing a 5-layer barrier.
- Understanding the role that trapped water plays in diffusion kinetics is important for our open-air plasma deposition as moisture is present in the atmosphere and maybe incorporated into the film.
- FTIR spectra reveals presence of water either trapped within or on the surface of the barrier.
- Using simple 1D diffusion principles, we show that the presence of water trapped within the film is negligible and not enough to influence the barrier properties of the film. There are two cases considered: 1. c_o (concentration of trapped water) ~ c_{atm} (concentration of water in the atmosphere) 2. c_o >> c_{atm}
- In case 1, the effect of the trapped water is not shown. In case 2, the effect of trapped water is present but only at very short time scales and results in a negligible amount of water penetration.
- WVTR derived from 1D diffusion modeling results in a similar WVTR value to the reported value.

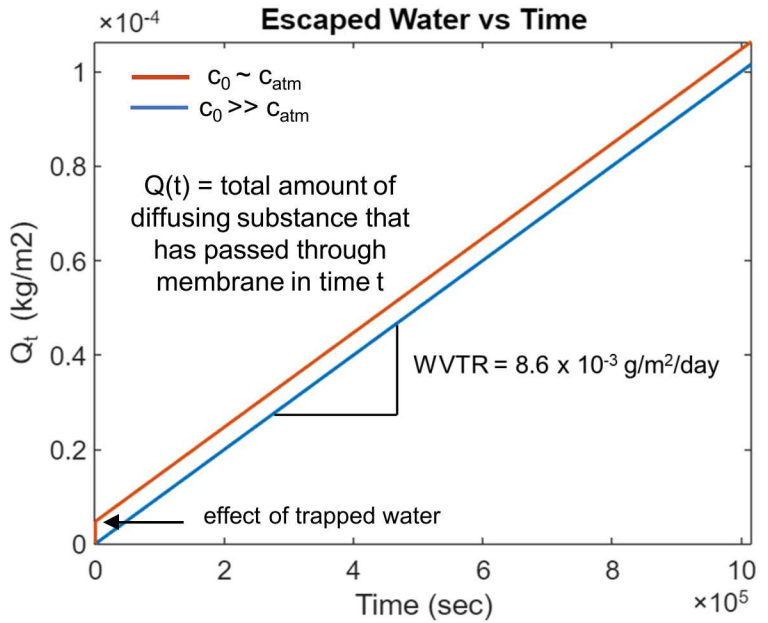

Quarterly Progress Update

Task 1 – Bifacial module materials degradation and interface reliability characterization:

- Development and assembly of the base bifacial mini-modules in coordination with our collaborators SolarTech Universal and Dupont in progress.

Task 2 – Develop and validate a transparent polymer back lamination technology with improved adhesion and moisture protection as a back-glass replacement:

- Have successfully demonstrated the WVTR of multi-dyad stack to have WVTR < 10^{-2} g/m^2/day in accelerated aging conditions of 38C and 90% RH.
- Open-air processing has significant advantages in reducing capital equipment costs, but films in open-air may have higher moisture content than those fabricated in dry environments.
- Modelled the influence of trapped water on barrier properties of our multilayer thin film barrier structure.
- Results of model suggest that trapped water in an open-air deposited barrier does not play an important role in barrier properties.

Low-Cost Advanced Metallization to Reduce Cell-Crack-Induced Degradation for Increased Module Reliability

PI: Sang M Han – Osazda Energy, LLC

Technology Summary and Impact

- Validated economic impact of crack resistant modules - TEA
- Optimize processing and composition of paste
- Perform Weibull Analysis to understand the relationship between crack size and failure probability

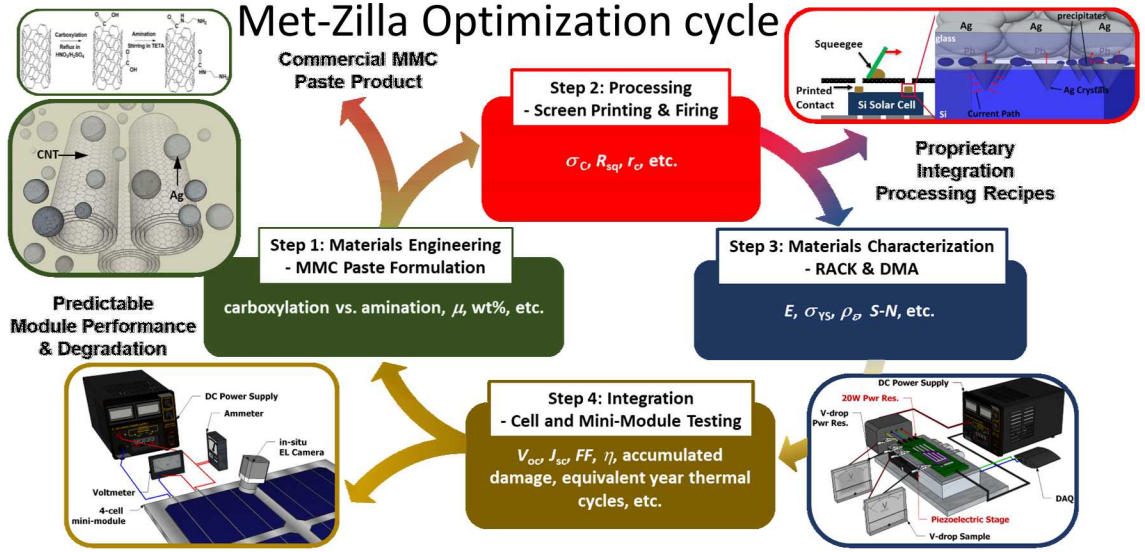

Resources

- P. Thornton, L. Schelhas, S. Moffitt, and R.H. Dauskardt. Fundamental Degradation Mechanisms for Reliability of PV Module Encapsulants, to be submitted to Progress in Photovoltaics.
- O. Zhao, Y. Ding, Z. Pan, N. Rolston, J. Zhang, and R.H. Dauskardt. Open-Air Plasma-Deposited Silica Films in a Multilayer Barrier for Improved Stability of Moisture Sensitive Devices. In review ACS Applied Materials and Interfaces.

Teaming

Team: Sang M Han/Osazda Energy, Ajeet Rohatgi/Gregoria Institute of Technology, Timothy Silverman/NREL, Nick Bosco/ NREL

Prior work: In Situ Scanning Electron Microscope (SEM) Strain Test

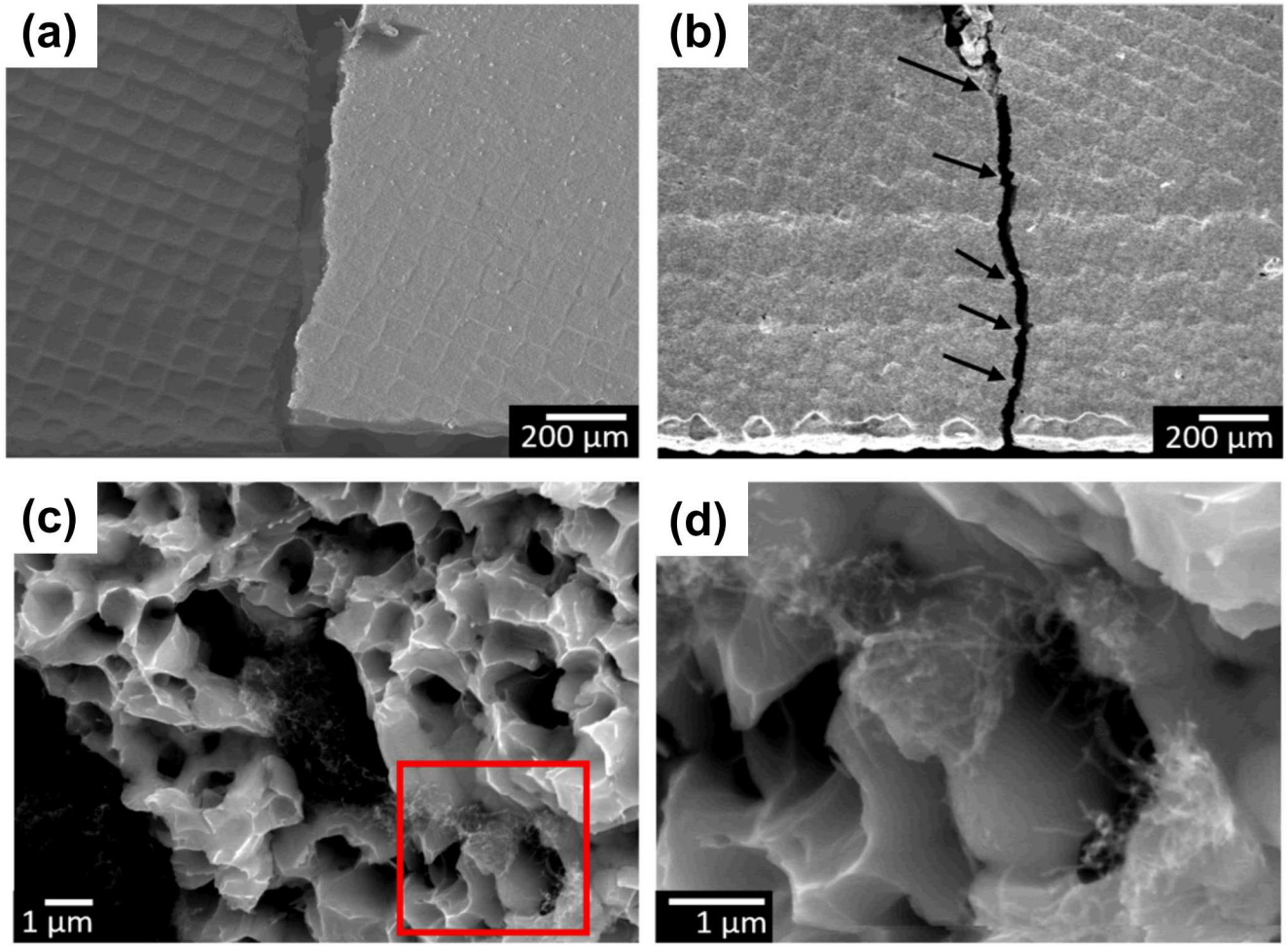

Figure 1: Fracture surfaces of printed and fired gridlines made from (a) commercial paste and (b) MetZilla™ metal matrix composite paste. (c and d) Fractured surface of composite gridlines shows a high level of extrusions/intrusions and reveals carbon nanotubes.

- Fractured surface of MetZilla™ metal matrix composite (MMC) gridlines shows microscopic extrusions/intrusions.
- Helps to maintain electrical continuity after the gridlines fracture, providing the gap-bridging capability.
- Asperities can also provide “self-healing” during crack closure.

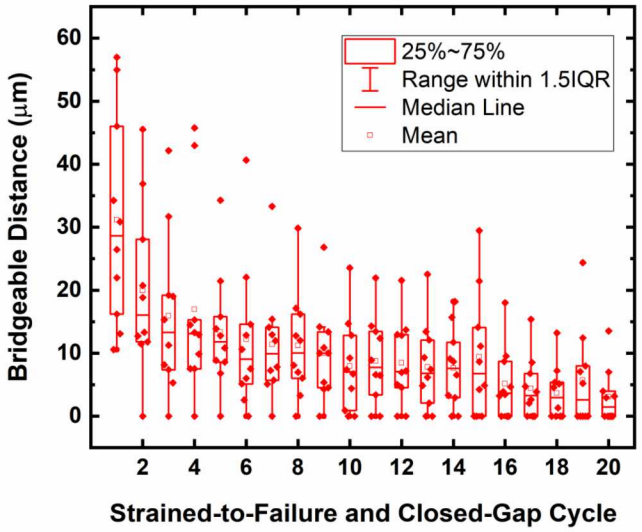

CNT Agglomerations vs. Weight % in Silver Paste (Osazda)

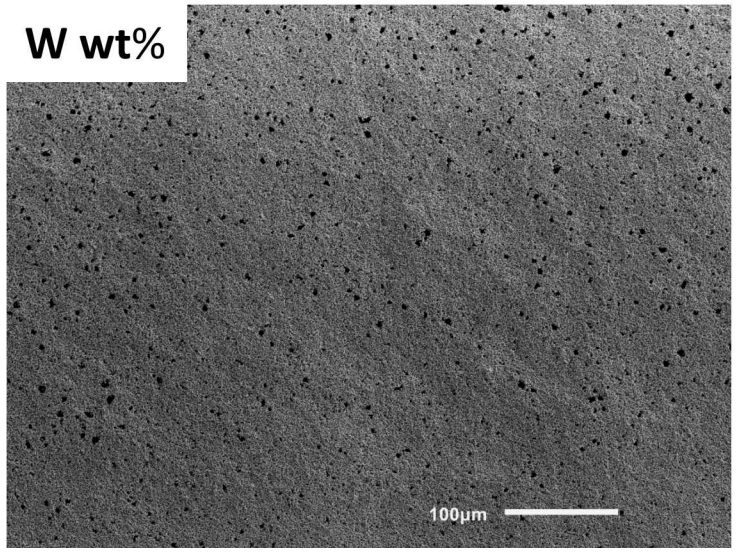

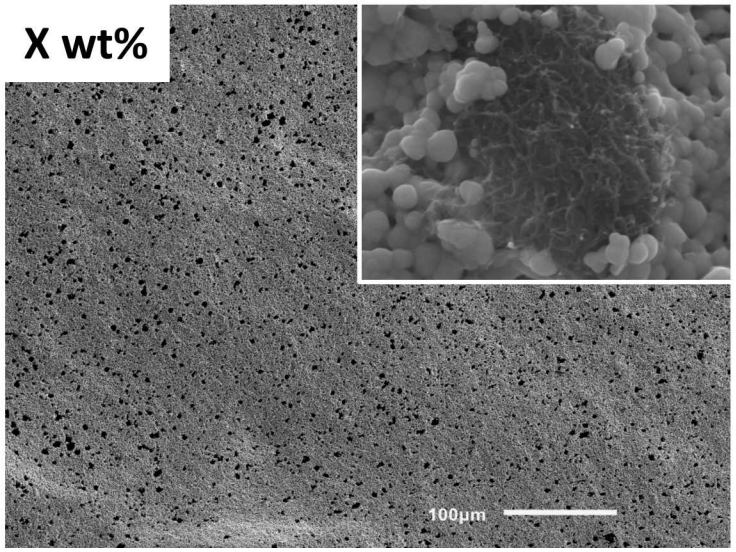

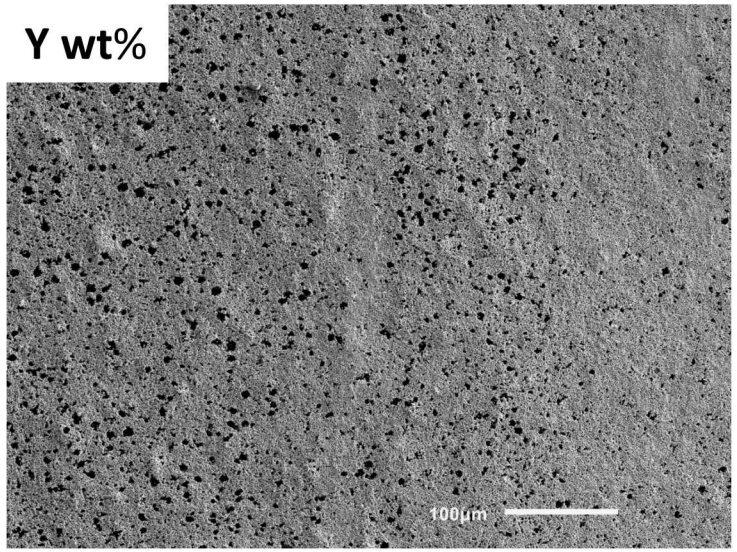

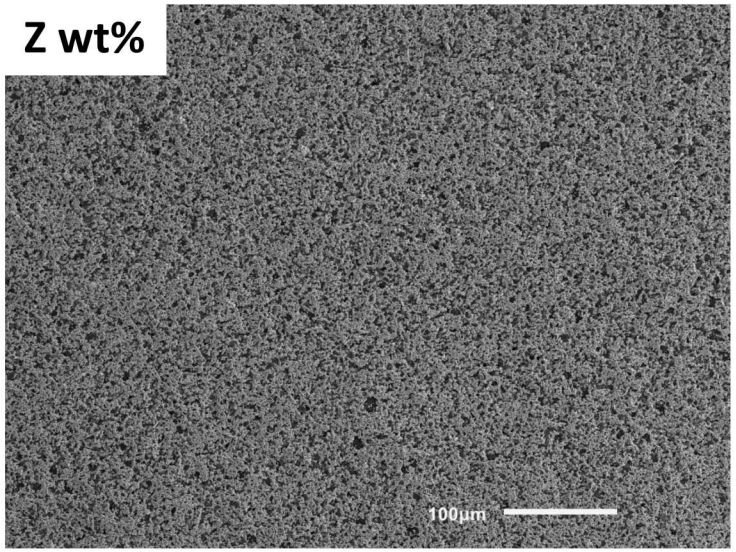

- ✓ Black dots in SEM images represent CNT agglomerates.
- ✓ CNT surface functionalization and polymer encapsulation determine effective activity coefficient (i.e., solubility) of CNTs in silver paste.
- ✓ Excess CNT loading (wt %) leads to increasing agglomerations and compromised mechanical properties.
- ✓ Additional optimization of CNT surface functionalization and dispersion (mechanical mixing) in silver paste appears necessary to eliminate or minimize CNT agglomerations.
- ✓ We expect to further improve composite material properties by improving CNT solubility and dispersion in silver paste.

Weibull Analysis of Short and Detangled CNTs in Silver Composite (Osazda)

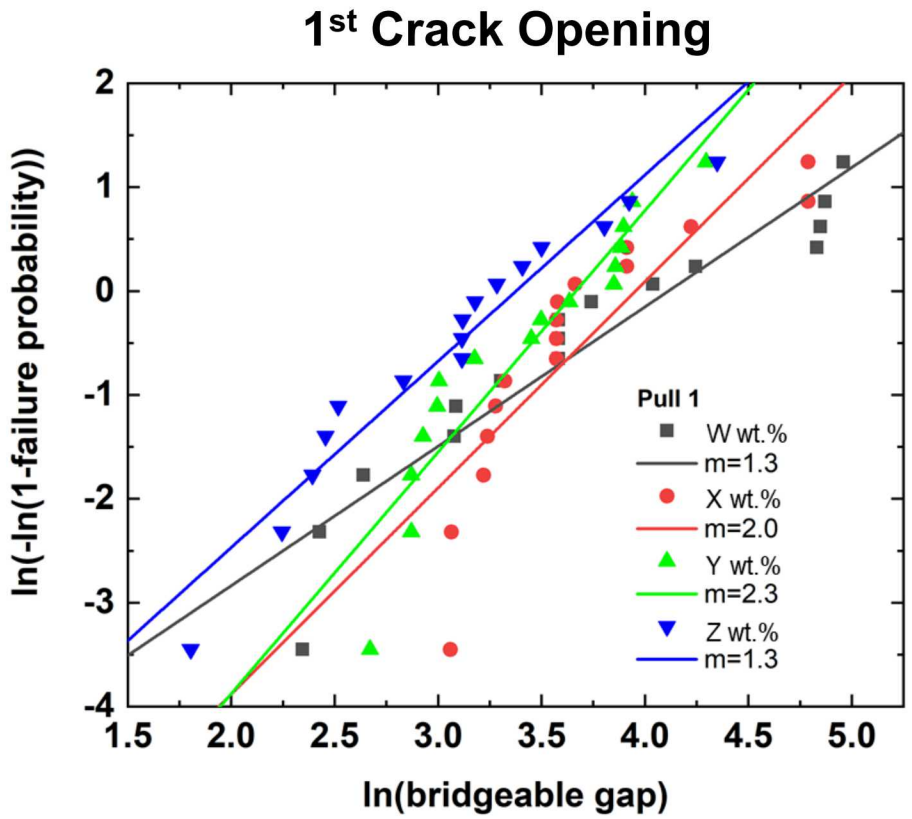

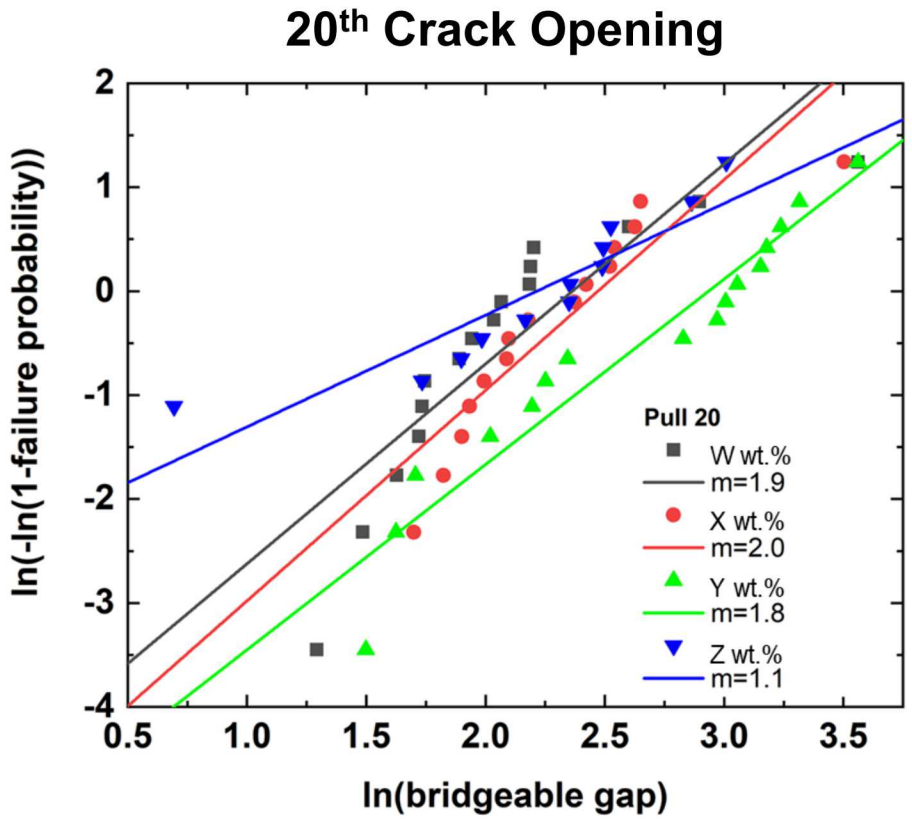

- ✓ 1st crack opening/electrical failure and 20th crack opening/electrical failure of composite metal gridlines during self-healing cycles show similar slopes, suggesting a similar failure mode type.
- ✓ Slope (i.e., Weibull modulus, also known as shape parameter, *m*) is relatively small, indicating a wide distribution of bridgeable gaps at which the composite metal lines electrically fail.
- ✓ Independent experiment and observation at NREL by Nick Bosco is very similar.

Standard and MetZilla™ Paste Materials Costs Calculation (M. Woodhouse)

Material	Consumption	Material Cost	Cost per cell
Frontside metallization paste for fingers and busbars	65 mg per cell	$550/kg	$0.0413
Backside tabbing metallization paste	22.5 mg per cell	$410/kg	$0.0092
Functionalized CNTs	1 mg per cell	$8,000/kg	$0.0080
Total Cost per Cell (M6=274.15 mm^2)		$0.0505 Standard PERC paste $0.0585 MetZilla paste	
Total Cost per Watt 22% Efficiency =6.0 W per cell		**$0.0084/W Standard PERC paste** **$0.0098 MetZilla paste**	

Trend for remaining Silver per cell incl. bus bars

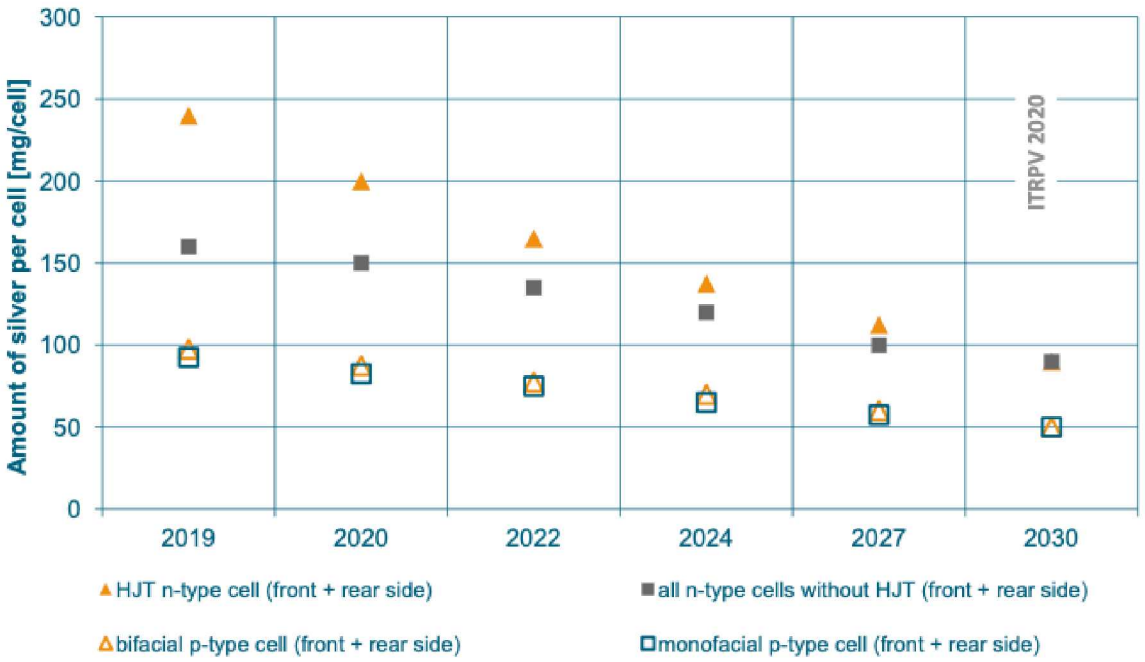

Total silver paste from 2020 ITRPV: 87.5 mg per cell

✓ CNT addition in MetZilla™ paste adds negligible cost ($0.0098/W) to module construction, while mitigating or potentially eliminating the cell-crack-related degradation.

Module Replacement Costs (M. Woodhouse)

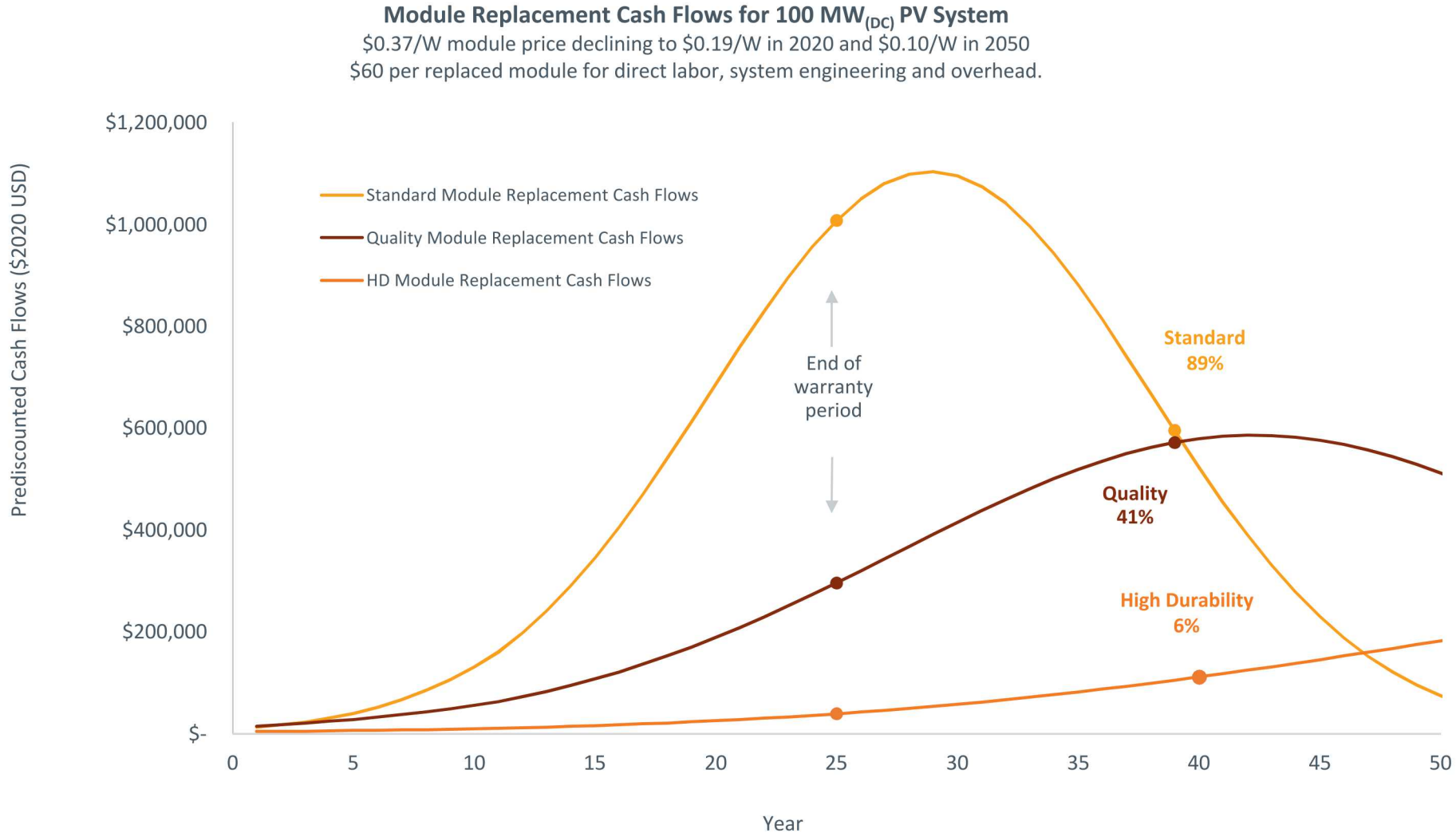

✓ Increased durability by reducing cell-crack-induced degradation would reduce module replacement costs, improving the cashflow for utility-scale PV projects.

BACKFLIP:Determination of BACKsheet material properties : a comparison of market-benchmark technologies to novel non-FLuoro-based co-extruded backsheet materials and their correlation and ImPact on PV module degradation rates PI: Kurt Van Durme /Nicola Siccheiri DSM Innovation

Technology Summary and Impact

- PV backsheet material durability under accelerated aging and outdoor weathering
  - Study a variety of co-extruded, fluorine-free backsheet materials, and compared to benchmark market backsheets, as-is, and when-utilized in a PV module
- General/advanced characterization, and forensics
- Derive parametrized equation of backsheets degradation rates and predicting the service life of backsheets, validated by both lab and outdoor testing.
- Final product lifetime prediction
- Suggestions for PV backsheet materials optimization
- A fast track PV module market adaptation for novel high-quality materials

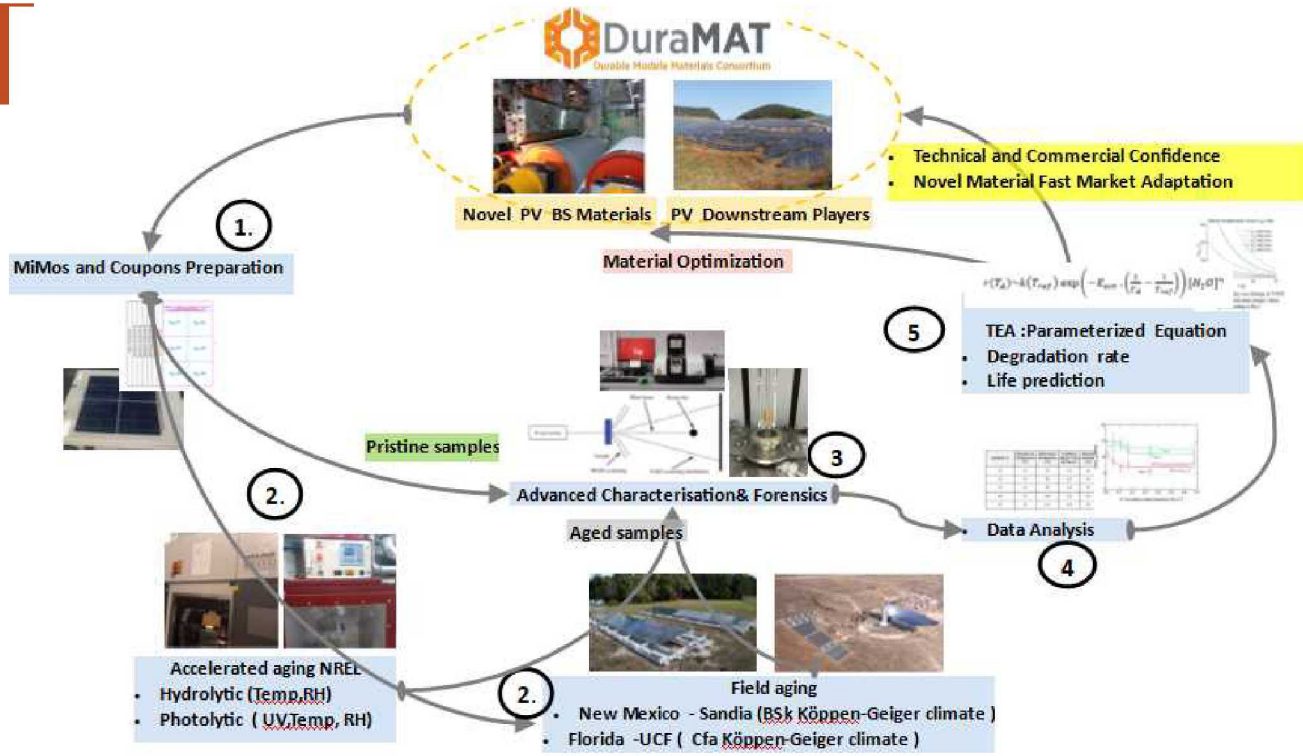

Teaming

Team: Laura T. Schelhas, Archana Sinha, Sona Ulicna, SLAC; Bruce King, Ashley Maes, Sandia; David Miller, NREL; Frederic Dross (until mid 2020) -> Nicola Siccheiri, Milica Mrcarica (until 2019) -> Kurt van Durme, Nicoleta Voicu, Peter Pasmans, Flanco Zhuge, Rob Janssen, DSM Innovation

25 Yr. Low LCOE Flexible PV Modules
PI: David Okawa – SunPower Corporation

Technology Summary and Impact

- Select the back layer and encapsulant to enable high efficiency, reliable, light-weight modules that enable direct to roof attach.
- Define the technical requirement of each component in the flexible module as well as the overall material stack
- Determine experimental plans to evaluate the performance degradation of he flexible module as well as calculate the lifetime of each material component.

Mission Profile

Residential
- Up to 85°C normal operating temperature
- Flowing water & debris
- Sliding snow

Commercial
- Up to 70°C normal operating temperature
- Standing water
- Heavy soil accumulation

Shared
- Mechanical: handling, dropping etc
- Hot spots, localized shading etc

Flexible vs Rigid Panel

	Rigid Panels	Flexible Panels
		
Pros	• Mechanical rigidity • Industry proven	• Direct-to-roof attach • Works on more roof structures • Lower shipping costs • Quicker installation • Higher ground coverage ratio
Cons	• Heavy • Mechanical balance of systems • Installation time & complexity	• Novel structure • Susceptible to mechanical stresses • Higher operating temperature • System tilt angle

Teaming

Team: David Okawa, Hoi Ng, Tami Lance, Samantha Hoang – Sunpower
Mike Kempe, Peter Hacke - NREL

Acknowledgements

NREL
NATIONAL RENEWABLE ENERGY LABORATORY
Sandia National Laboratories
ASU Arizona State University
Stanford University
The University of Akron
Georgia Tech
CUNY THE CITY UNIVERSITY OF NEW YORK
Colorado State University
EPRI ELECTRIC POWER RESEARCH INSTITUTE
DSM
BRIGHT SCIENCE. BRIGHTER LIVING.
osazda ENERGY
SUNPOWER
WattGlass
Lawrence Livermore National Laboratory
SLAC NATIONAL ACCELERATOR LABORATORY
BERKELEY LAB

DuraMAT's Industry Advisory Board